

# Forecasting range shifts of a dioecious plant species under climate change

Jacob K. Moutouama 0000-0003-1599-1671<sup>\*1</sup>, Aldo Compagnoni 0000-0001-8302-7492<sup>2</sup>, and Tom E.X. Miller 0000-0003-3208-6067<sup>1</sup>

<sup>1</sup>Program in Ecology and Evolutionary Biology, Department of BioSciences, Rice University, Houston, Texas, USA

<sup>2</sup>Institute

of Biology, Martin Luther University Halle-Wittenberg, Halle, Germany; and German Centre for Integrative Biodiversity Research (iDiv), Leipzig, Germany

**Running header:** Forecasting range shifts

**Keywords:** demography, forecasting, global warming, matrix projection model, population dynamics, sex ratio, range limits

**Submitted to:** *Ecology letters* (Letter)

**Data accessibility statement:** All data used in this paper are publicly available and cited appropriately (?). Should the paper be accepted, all computer scripts supporting the results will be archived in a Zenodo package, with the DOI included at the end of the article. During peer review, our code (Stan and R) is available at <https://github.com/jmoutouama/POAR-Forecasting>.

**Conflict of interest statement:** None.

**Authorship statement:** J.K.M., A.C. and T.E.X.M. designed the study. A.C. and T.E.X.M. collected the data. All authors conducted the statistical analyses and modeling. J.K.M. drafted the manuscript, and T.E.X.M contributed to revisions.

**Abstract:**

**Main Text:**

**Figures:** 6

**Tables:** 0

**References:** 106

---

\*Corresponding author: jmoutouama@gmail.com

## **1 Abstract**

2 Global climate change has triggered an urgent need for predicting the reorganization of Earth's  
3 biodiversity. Currently, the vast majority of models used to forecast population viability and  
4 range shifts in response to climate change ignore the complication of sex structure, and thus  
5 the potential for females and males to differ in their sensitivity to climate drivers. We developed  
6 demographic models of range limitation, parameterized from geographically distributed com-  
7 mon garden experiments, with females and males of a dioecious grass species (*Poa arachnifera*)  
8 throughout and beyond its range in the south-central U.S. Female-dominant and two-sex  
9 model versions both predict that future climate change will alter population viability and  
10 will induce a poleward niche shift beyond current northern limits. However, the magnitude of  
11 niche shift was underestimated by the female-dominant model, because females have broader  
12 temperature tolerance than males and become mate-limited under female-biased sex ratios.  
13 Our result illustrate how explicit accounting for both sexes could enhance population viability  
14 forecasts and conservation planning for dioecious species in response to climate change.

15 **Introduction**

16 Rising temperatures and extreme drought events associated with global climate change are  
17 leading to increased concern about how species will become redistributed across the globe  
18 under future climate conditions (??). Species' range limits, when not driven by dispersal  
19 limitation, should generally reflect the limits of the ecological niche (?). Niches and geographic  
20 ranges are often limited by climatic factors including temperature and precipitation (?).  
21 Therefore, any substantial changes in the magnitude of these climatic factors could impact  
22 population viability, with implications for range expansions or contractions based on which  
23 regions of a species' range become more or less suitable (??).

24 Forecasting range shifts for dioecious species (most animals and ca. 7% of plant species)  
25 is complicated by the potential for sexual niche differentiation, i.e. distinct responses of females  
26 and males to shared climate drivers (????). The lower cost of reproduction for one sex (male or  
27 female) may allow that sex to invest its energy in other functions that produce higher growth  
28 rates, greater clonality, or even higher survival rates compared to the other sex, leading to sex-  
29 ual niche differentiation (?). Accounting for sexual niche differentiation is a long-standing chal-  
30 lenge in accurately predicting which sex will successfully track environmental change and how  
31 this will impact population viability and range shifts (??). Populations in which males are rare  
32 under current climatic conditions could experience low reproductive success due to sperm or  
33 pollen limitation that may lead to population decline in response to climate change that dispro-  
34 portionately favors females (?). In contrast, climate change could expand male habitat suitabil-  
35 ity (e.g. upslope movement), which might increase seed set for mate-limited females and favor  
36 range expansion (?). Across dioecious plants, for example, studies suggest that future climate  
37 change toward hotter and drier conditions may favor male-biased sex ratios (??). Although the  
38 response of species to climate warming is an urgent and active area of research, few studies  
39 have disentangled the interaction between sex and climate drivers to understand their com-  
40 bined effects on population dynamics and range shifts, despite calls for such an approach (??).

41 The vast majority of theory and models in population biology, including those used  
42 to forecast biodiversity responses to climate change, ignore the complication of sex structure  
43 (but see ???). Traditional approaches instead focus exclusively on females, assuming that  
44 males are in sufficient supply as to never limit female fertility. In contrast, "two-sex" models  
45 are required to fully account for demographic differences between females and males  
46 and sex-specific responses to shared climate drivers (??). Sex differences in maturation,  
47 reproduction, and mortality schedules can generate skew in the operational sex ratio (OSR;  
48 sex ratio of individuals available for mating) even if the birth sex ratio is 1:1 (??). Climate and  
49 other environmental drivers can therefore influence the OSR via their influence on sex-specific

50 demographic rates. In a two-sex framework, demographic rates both influence and respond  
51 to the OSR in a feedback loop that makes two-sex models inherently nonlinear and more  
52 data-hungry than corresponding female-dominant models. Given the additional complexity  
53 and data needs, forecasts of range dynamics for dioecious species under future climate change  
54 that explicitly account for females, males, and their inter-dependence are limited (??).

55 Tracking the impact of climate change on population viability ( $\lambda$ ) and distributional  
56 limits of dioecious taxa depends on our ability to build mechanistic models that take  
57 into account the spatial and temporal context of sex specific response to climate change,  
58 while accounting for sources of uncertainty (??). Structured population models built from  
59 demographic data collected from geographically distributed observations or common garden  
60 experiments provide several advantages for studying the impact of climate change on species'  
61 range shifts (???). First, demographic models link individual-level life history events (mortality,  
62 development, and regeneration) to population demography, allowing the investigation of  
63 factors explaining vital rate responses to environmental drivers (???). Second, demographic  
64 models have a natural interface with statistical estimation of individual-level vital rates  
65 that provide quantitative measures of uncertainty and isolate different sources of variation,  
66 features that can be propagated to population-level predictions (??). Finally, structured  
67 demographic models can be used to identify which aspects of climate are the most important  
68 drivers of population dynamics. For example, Life Table Response Experiments (LTRE) built  
69 from structured models have become widely used to understand the relative importance of  
70 covariates in explaining variation in population growth rate (???).

71 In this study, we combined geographically-distributed common garden experiments,  
72 hierarchical Bayesian statistical modeling, two-sex population projection modeling, and  
73 climate back-casting and forecasting to understand demographic responses to climate change  
74 and their implications for past, present, and future range dynamics. Our work focused on  
75 the dioecious plant Texas bluegrass (*Poa arachnifera*), which is distributed along environmental  
76 gradients in the south-central U.S. corresponding to variation in temperature across latitude  
77 and precipitation across longitude (Fig. 1A)<sup>1</sup>. This region has experienced rapid climate  
78 warming since 1900 and this is projected to continue through the end of the century (Fig. 1 B  
79 and C). Our previous study showed that, despite evidence for differentiation of climatic niche  
80 between sexes, the female niche mattered the most in driving longitudinal range limits of  
81 Texas bluegrass (?). However, that study used a single proxy variable (longitude) to represent  
82 environmental variation related to aridity and did not consider variation in temperature,  
83 which is the much stronger dimension of forecasted climate change in this region (Fig. S-2).  
84 Developing a rigorous forecast for the implications of future climate change requires that

---

<sup>1</sup>Fig. A does not show what we are saying here. Maybe I should add the Figure with the raster

85 we transition from implicit to explicit treatment of multiple climate drivers, as we do here.  
86 Leveraging the power of Bayesian inference, we take a probabilistic view of past, present,  
87 and future range limits by quantifying the probability of population viability ( $Pr(\lambda \geq 1)$ ) in  
88 relation to climate drivers of demography, an approach that fully accounts for uncertainty  
89 arising from multiple sources of estimation and process error. Specifically, we asked:  
90 1. What are the sex-specific vital rate responses to variation in temperature and precipitation  
91 across the species' range?  
92 2. How do sex-specific vital rates combine to determine the influence of climate variation  
93 on population growth rate ( $\lambda$ )?  
94 3. What is the impact of climate change on operational sex ratio throughout the range?  
95 4. What are the likely historical and projected dynamics of the Texas bluegrass geographic  
96 niche and how does accounting for sex structure modify these predictions?

## 97 Materials and methods

### 98 Study species and climate context

99 Texas bluegrass (*Poa arachnifera*) is a dioecious perennial, summer-dormant cool-season (C3)  
100 grass that occurs in the south-central U.S. (Texas, Oklahoma, and southern Kansas) (Figure  
101 1) (?). Texas bluegrass grows between October and May, flowers in spring, and goes dormant  
102 during the hot summer months of June to September (?). Following this life history, we  
103 divided the calendar year into growing (October 1 - May 31) and dormant (June 1 - September  
104 30) seasons in the analyses below. Biological sex is genetically based and the birth (seed)  
105 sex ratio is 1:1 (?). Females and males are morphologically indistinguishable except for their  
106 inflorescences. Like all grasses, this species is wind pollinated (?) and most male-female  
107 pollen transfer occurs within 10-15m (?). Surveys of 22 natural populations throughout the  
108 species' distribution indicated that operational sex ratio (the female fraction of inflorescences)  
109 ranged from 0.007 to 0.986 with a mean of 0.404 (?).

110 Latitudinal limits of the Texas bluegrass distribution span 7.74 °C to 16.94 °C of  
111 temperature during the dormant season and 24.38 °C to 28.80 °C during the dormant season.  
112 Longitudinal limits span 244.9 mm to 901.5 mm of precipitation during the growing season  
113 and 156.3 mm to 373.3 mm. This region has experienced *ca.* 0.5 °C of climate warming since  
114 1900, with faster warming during the cool-season months (0.0055°C/yr) than the hot summers  
115 (0.0046°C/yr) (Fig. S-1). Future warming is projected to accelerate to 0.03 – 0.06°C/yr by  
116 the end of the century depending on the season and forecast model. On the other hand,

<sup>117</sup> precipitation has increased over the past century for much of the region but is forecasted  
<sup>118</sup> to decline back to early-20th century levels (Fig. S-1). <sup>2</sup>

<sup>119</sup> **Common garden experiment**

<sup>120</sup> **Experimental design**

<sup>121</sup> We conducted a range-wide common garden experiment to quantify sex-specific demographic  
<sup>122</sup> responses to climate variation. Details of the experimental design are provided in ?; we provide  
<sup>123</sup> a brief overview here. The experiment was installed at 14 sites throughout and, in some  
<sup>124</sup> cases, beyond the natural range of Texas bluegrass that sampled a broad range of latitude and  
<sup>125</sup> longitude (Figure 1A). At each site, we established 14 blocks. For each block we planted three  
<sup>126</sup> female and three male individuals that were clonally propagated from females and males from  
<sup>127</sup> eight natural source populations (Figure 1A); because sex is genetically-based, clones never  
<sup>128</sup> deviated from their expected sex. The experiment was established in November 2013 with  
<sup>129</sup> a total of 588 female and 588 male plants, and was censused in May of 2014, 2015, and 2016.  
<sup>130</sup> At each census, we collected data on survival, size (number of tillers), and number of panicles  
<sup>131</sup> (reproductive inflorescences). For the analyses that follow, we focus on the 2014-15 and 2015-16  
<sup>132</sup> transition years, since the start of the experiment did not include the full 2013-14 transition year.

---

<sup>2</sup>*I like this but I don't know if this not a repetition of what we've said in the introduction about climate change in the study area.*

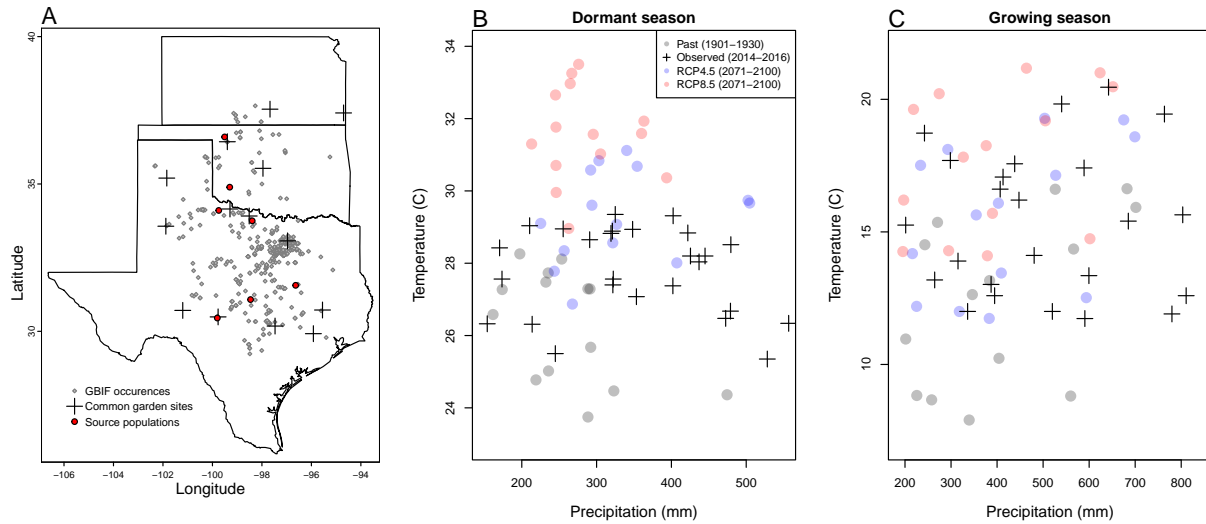


**Figure 1: Experimental gardens and climate of the study region.** **A:** Map of 14 experimental garden sites (crosses) in Texas, Oklahoma, and Kansas relative to GBIF occurrences of *Poa arachnifera* (gray points). Red points indicate source populations for plants used in the common garden experiment. **B,C:** Past, future, and observed climate space for growing and dormant seasons. Crosses show observed conditions for the sites and years of the common garden experiment. Gray points show historical (1901-1930) climate normals, and blue and red points show end-of-century (2071-2100) climate normals for RCP4.5 and RCP8.5 projections, respectively, from MIROC5. See also (Figure ?? for more information about historical and projected climate change in the study region.

### 133 Climatic data collection

134 We gathered downscaled monthly temperature and precipitation for each site from Chelsa (?)  
 135 to describe observed climate conditions during our study period. These climate data were used  
 136 as covariates in vital rate regressions. We aligned the climatic years to match demographic tran-  
 137 sition years (June 1 – May 31) and growing and dormant seasons within each year. To back-cast  
 138 and forecast demographic responses to changes in climate throughout the study region, we also  
 139 gathered projection data for three 30-year periods: “past” (1901-1930), “current” (1990-2019)  
 140 and “future” (2070-2100). Data for future climatic periods were downloaded from four general  
 141 circulation models (GCMs) selected from the Coupled Model Intercomparison Project Phase 5  
 142 (CMIP5): Model for Interdisciplinary Research on Climate (MIROC5), Australian Community  
 143 Climate and Earth System Simulator (ACCESS1-3), Community Earth System Model (CESM1-  
 144 BGC), Centro Euro-Mediterraneo sui Cambiamenti Climatici Climate Model (CMCC-CM). All  
 145 the GCMs were also downloaded from Chelsa (?). We evaluated future climate projections from  
 146 two scenarios of representative concentration pathways (RCPs): RCP4.5, an intermediate-to-  
 147 pessimistic scenario assuming a radiative forcing amounting to  $4.5 \text{ W m}^{-2}$  by 2100, and RCP8.5,  
 148 a pessimistic emission scenario which projects a radiative forcing of  $8.5 \text{ W m}^{-2}$  by 2100 (??).

149 Projection data for the three 30-year periods included warmer or colder conditions than ob-  
150 served in our experiment, so extending our inferences to these conditions required some extrap-  
151 olation. However, across all sites, both study years were 1-2°C warmer than their correspond-  
152 ing “current” (1990-2019) temperature normals (Fig. S-2). Additionally, the 2014–15 growing  
153 season was generally wetter and cooler across the study region than 2015–16 (Fig. S-2). Com-  
154 bined, the geographic and inter-annual replication of the common garden experiment provided  
155 good coverage of most past and future conditions throughout the study region (Fig. 1B,C).

156 **Sex-specific demographic responses to climatic variation across common garden sites**

157 We used individual-level measurements of survival, growth (change in number of tillers), flow-  
158 ering, and number of panicles (conditional on flowering) to develop Bayesian mixed effect mod-  
159 els describing how each vital rate varies as a function of sex, size, and four climate covariates  
160 (precipitation and temperature of growing and dormant season)(Supplementary Method S.2.1).  
161 These vital rate models included main effects of size (the natural log of tiller number), sex, and  
162 seasonal climate covariates. Climate variables were fit with second-degree polynomial func-  
163 tions to accommodate the possibility of hump-shaped relationships (reduced demographic per-  
164 formance at both extremes). We also included two-way interactions between sex and each cli-  
165 mate driver and between temperature and precipitation within each season, and a three-way in-  
166 teraction between sex, temperature, and precipitation within each season. We modeled survival  
167 and flowering data with a Bernoulli distribution and the growth (tiller number) with a zero-  
168 truncated Poisson inverse Gaussian distribution. Fertility (panicle count conditional on flower-  
169 ing) was modeled as zero-truncated negative binomial. We used generic, weakly informative  
170 priors to fit coefficients for survival, growth, flowering models ( $\beta \sim N(0, 1.5)$ ) and random  
171 effect variances ( $\sigma \sim Gamma(\gamma(0.1, 0.1))$ ). We fit fertility model with also weakly informative pri-  
172 ors for coefficients ( $\beta \sim N(0, 0.15)$ ). Different priors were used for fertility because the panicle  
173 model has a large number of parameters relative to the amount of available data (subset of our  
174 data) and because these specifics priors help prevent the model from overfitting. Each vital rate  
175 also includes normally distributed random effects for block-to-block variation ( $\phi \sim N(0, \sigma_{block})$ ),  
176 site to site variation ( $\nu \sim N(0, \sigma_{site})$ ), and source-to-source variation that is related to the genetic  
177 provenence of the transplants used to establish the common garden ( $\rho \sim N(0, \sigma_{source})$ ).

178 **Sex ratio responses to climatic variation across common garden sites**

179 We also used the experimental data to investigate how climatic variation across the range  
180 influenced sex ratio and operational sex ratio of the common garden populations. To do so,  
181 we developed two Bayesian linear models using data collected during three years. Each model

had OSR or SR as response variable and a climate variable (temperature and precipitation of the growing season and dormant season) as predictor (Supplementary Method S.2.2). We modeled the OSR or SR data with a Bernoulli distribution and used non informative priors for each coefficient ( $\omega \sim N(0, 100)$ ).

## Model-fitting procedures

All models were fit using Stan (?) in R 4.3.1 (?). We centered and standardized all climatic predictors to mean zero, variance one, which facilitated model convergence. We ran three chains for 1000 samples for warmup and 4000 for sampling, with a thinning rate of 3. We assessed the quality of the models using posterior predictive checks (?) (Figure S-3).

## Two-sex and female-dominant matrix projection models

We used the climate-dependent vital rate regressions estimated above, combined with additional data sources, to build female-dominant and two-sex versions of a climate-explicit matrix projection model (MPMs) structured by the discrete state variables size (number of tillers) and sex. The female-dominant and two-sex versions of the model both allow for sex-specific response to climate and differ only in the feedback between operational sex ratio and seed fertilization. For clarity of presentation we do not explicitly include climate-dependence in the notation below, but the following model was evaluated over variation in seasonal temperature and precipitation.

Let  $F_{x, t}$  and  $M_{x, t}$  be the number of female and male plants of size  $x$  in year  $t$ , where  $x \in [1, \dots, U]$ . The minimum possible size is one tiller and  $U$  is the 95th percentile of observed maximum size (35 tillers). Let  $F_t^R$  and  $M_t^R$  be new female and male recruits in year  $t$ , which we treat as distinct from the rest of the size distribution because we assume they do not reproduce in their first year, consistent with our observations. For a pre-breeding census, the expected numbers of recruits in year  $t+1$  is given by:

$$F_{t+1}^R = \sum_1^U [p^F(x) \cdot c^F(x) \cdot d \cdot v(\mathbf{F}_t, \mathbf{M}_t) \cdot m \cdot \rho] F_{x, t} \quad (1)$$

$$M_{t+1}^R = \sum_1^U [p^F(x) \cdot c^F(x) \cdot d \cdot v(\mathbf{F}_t, \mathbf{M}_t) \cdot m \cdot (1 - \rho)] F_{x, t} \quad (2)$$

where  $p^F$  and  $c^F$  are flowering probability and panicle production for females of size  $x$ ,  $d$  is the number of seeds per female panicle,  $v$  is the probability that a seed is fertilized,  $m$  is the probability that a fertilized seed germinates, and  $\rho$  is the primary sex ratio (proportion of recruits that are female), which we assume to be 0.5 (?).

212 In the two-sex model, seed fertilization is a function of population structure, allowing for  
 213 feedback between vital rates and operational sex ratio (OSR). In the context of the model, OSR  
 214 is defined as the fraction of panicles that are female and is derived from the  $U \times 1$  vectors  
 215  $\mathbf{F}_t$  and  $\mathbf{M}_t$ :

$$216 v(\mathbf{F}_t, \mathbf{M}_t) = v_0 * \left[ 1 - \left( \frac{\sum_1^U p^F(x, z) c^F(x, z) F_{x,t}}{\sum_1^U p^F(x, z) c^F(x, z) F_{x,t} + p^M(x, z) c^M(x, z) M_{x,t}} \right)^\alpha \right] \quad (3)$$

217 The summations tally the total number of female and male panicles over the size distribution,  
 218 giving the fraction of total panicles that are female. We focus on the female fraction of  
 219 panicles and not female fraction of reproductive individuals because panicle number can vary  
 220 widely depending on size; we assume that few males with many panicles vs. many males  
 221 with few panicles are interchangeable pollination environments. Eq. 3 has the properties  
 222 that seed fertilization is maximized at  $v_0$  as OSR approaches 100% male, goes to zero as  
 223 OSR approaches 100% female, and parameter  $\alpha$  controls how female seed viability declines  
 224 as male panicles become rare. We estimated these parameters using data from a sex ratio  
 225 manipulation experiment, conducted in the center of the range, in which seed fertilization  
 226 was measured in plots of varying OSR; this experiment is described elsewhere (?) and is  
 227 summarized in **Supplementary Method S.2.3**<sup>3</sup>. This experiment also provided estimates for  
 228 seed number per panicle ( $d$ ) and germination rate ( $m$ ). Lacking data on climate-dependence,  
 229 we assume that seed fertilization, seed number, and germination rate do not vary with climate.

230 The dynamics of the size-structured component of the population are given by:

$$231 F_{y,t+1} = [\sigma \cdot g^F(y, x=1)] F_t^R + \sum_L^U [s^F(x) \cdot g^F(y, x)] F_{x,t} \quad (4)$$

$$232 M_{y,t+1} = [\sigma \cdot g^M(y, x=1)] M_t^R + \sum_L^U [s^M(x) \cdot g^M(y, x)] M_{x,t} \quad (5)$$

233 The first terms indicate recruits that survived their first year and enter the size distribution  
 234 of established plants. We estimated the seedling survival probability  $\sigma$  using demographic  
 235 data from the congeneric species *Poa autumnalis* in east Texas (T.E.X. Miller and J.A. Rudgers,  
 236 *unpublished data*), and we assume that  $\sigma$  is the same across sexes and climatic variables. We did  
 237 this because we had little information on the early life cycle transitions of greenhouse-raised  
 238 transplants. We used  $g(y, x=1)$  (the future size distribution of one-tiller plants from the  
 239 transplant experiment) to give the probability that a surviving recruit reaches size  $y$ . The  
 240 second component of the equations indicates survival and size transition of established

---

<sup>3</sup>I think the supplement should also include a data figure showing the fit of the model to the experimental data.

241 plants from the previous year, where  $s$  and  $g$  give the probabilities of surviving at size  $x$  and  
242 growing from sizes  $x$  to  $y$ , respectively, and superscripts indicate that these functions may  
243 be unique to females ( $F$ ) and males ( $M$ ).

244 The model described above yields a  $2(U+1) \times 2(U+1)$  transition matrix. We estimated  
245 the population growth rate  $\lambda$  of the female dominant model as the leading eigenvalue of  
246 the transition matrix. Since the two-sex MPM is nonlinear (matrix elements affect and are  
247 affected by population structure) we estimated  $\lambda$  and stable sex ratio (female fraction of all  
248 individuals) and operational sex ratio (female fraction of panicles) by numerical simulation.  
249 Since all parameters were estimated using MCMC sampling, we were able to propagate the  
250 uncertainty in our estimates of the vital rate parameters to uncertainty in  $\lambda$ . Furthermore,  
251 by sampling over distributions associated with site, block, and source population variance  
252 terms, we are able to incorporate process error into the total uncertainty in  $\lambda$ , in addition  
253 to the uncertainty that arises from imperfect knowledge of the parameter values. For example,  
254 sampling over site and block variances accounts for regional and local spatial heterogeneity  
255 that is not explained by climate, and sampling over source population variance accounts for  
256 genetically-based demographic differences across the species' range.

## 257 Life Table Response Experiments

258 We conducted two types of Life Table Response Experiments (LTRE) to isolate contributions  
259 of climate variables and sex-specific vital rates to variation in  $\lambda$ . First, to identify which  
260 aspect of climate is most important for population viability, we used an LTRE based on  
261 a nonparametric model for the dependence of  $\lambda$  on parameters associated with seasonal  
262 temperature and precipitation (?). To do so, we used the RandomForest package to fit a  
263 regression model with four climatic variables (temperature of growing season, precipitation of  
264 growing season, temperature of the dormant season and precipitation of the dormant season)  
265 as predictors and  $\lambda$  calculated from the two sex model as response (?). The regression model  
266 allowed the estimation of the relative importance of each predictor.

267 Second, to understand how climate drivers influence  $\lambda$  via sex-specific demography, we  
268 decomposed the effect of each climate variable on population growth rate ( $\lambda$ ) into contribution  
269 arising from the effect on each female and male vital rate using a "regression design" LTRE  
270 (??). This LTRE decomposes the sensitivity of  $\lambda$  to climate according to:

$$\frac{\partial \lambda}{\partial \text{climate}} \approx \sum_i \frac{\partial \lambda}{\partial \theta_i^F} \frac{\partial \theta_i^F}{\partial \text{climate}} + \frac{\partial \lambda}{\partial \theta_i^M} \frac{\partial \theta_i^M}{\partial \text{climate}} \quad (6)$$

272 where,  $\theta_i^F$  and  $\theta_i^M$  represent sex-specific parameters (the regression coefficients of the vital  
273 rate functions). Because LTRE contributions are additive, we summed across vital rates to  
274 compare the total contributions of female and male parameters.<sup>45</sup>

## 275 Population viability across the climatic niche and geographic range

276 To understand how climate shapes the niche and geographic range of Texas bluegrass, we  
277 estimated the probability of self-sustaining populations ( $\Pr(\lambda \geq 1)$ ) conditional to temperature  
278 and precipitation of the dormant and growing seasons.  $\Pr(\lambda > 1)$  was calculated for the  
279 two-sex model and the female dominant MPMs using the proportion of the 300 posterior  
280 samples that lead to a  $\lambda \geq 1$  (?). Population viability in climate niche space was then  
281 represented as a contour plot with values of  $\Pr(\lambda > 1)$  at given temperature and precipitation  
282 for the growing season, holding dormant season climate constant, and vice versa.

283  $\Pr(\lambda > 1)$  was also mapped onto geographic layers of three US states (Texas, Oklahoma  
284 and Kansas) to delineate past, current and future potential geographic distribution of the  
285 species. To do so, we estimated  $\Pr(\lambda > 1)$  conditional to all climate covariates for each  
286 pixel ( $\sim 25 \text{ km}^2$ ) for each time period (past, present, future). Because of the amount of the  
287 computation involved, we use 100 posterior samples to estimate  $\Pr(\lambda > 1)$  across the study  
288 area (Texas, Oklahoma and Kansas).

## 289 Results

### 290 Sex specific demographic response and sex ratio variation across climatic 291 conditions

292 We found strong demographic responses to climate drivers across our Texas bluegrass  
293 common garden sites and years, and evidence for demographic differences between the sexes.  
294 Regression coefficients related to sex and/or sex:size interactions were significantly non-zero  
295 (95% credible intervals excluding zero) for most vital rates (Fig. S-4), suggesting sexual  
296 divergence in demography. Females generally had an advantage over males, especially in  
297 survival and flowering (Fig. 2). That female demographic advantage was more pronounced for

---

<sup>4</sup>Let's talk about this

<sup>5</sup>I do not agree. It is true that you can compute this, but only by "turning off" the interaction by holding the interacting variable constant. I still think this needs to be better addressed in both LTRE analyses.

298 extreme values of climate (Fig. S-5, Fig. S-6).<sup>6</sup> Vital rate regressions also revealed significant  
 299 interactions between sex and climate drivers, especially in vegetative growth (Fig. S-4)B.<sup>7</sup>

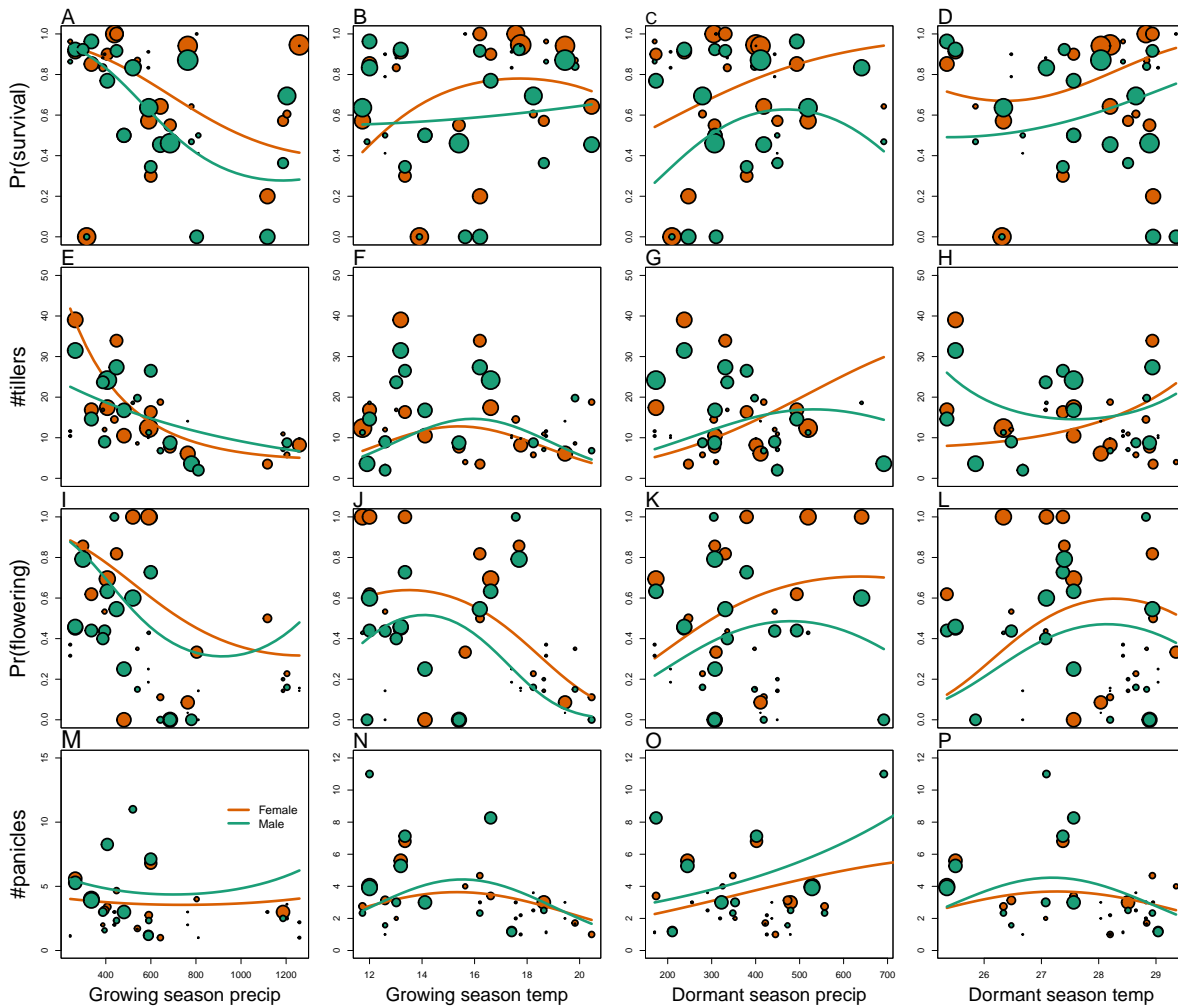


**Figure 2: Sex specific demographic response to climate across species range.** (A, B, C, D) Probability of survival as a function of precipitation and temperature of the growing and dormant season. (E, F, G, H) Change in number of tillers as a function of precipitation and temperature of the growing and dormant season. (I, J, K, L) Probability of flowering as a function of precipitation and temperature of growing and dormant season. (M, N, O, P) Change in number of panicles as a function of precipitation and temperature of the growing and dormant season. Points show means by site for females (orange) and males (green). Points sizes are proportional to the sample sizes of the mean and are jittered. Lines show fitted statistical models for females (orange) and males (green) based on posterior mean parameter values.

300 Across common garden sites, operational sex ratio (proportion of female panicles) of the  
 301 experimental populations was female-biased on average (STATS), reflecting the overall greater

<sup>6</sup>I added the 3D plots for vital rates to show that female individuals do better in extreme climate

<sup>7</sup>I am skipping the rest of this section for now because I think we need a different visualization for the vital rates. I also think this section should include the common garden sex ratio results, since they are connected to the vital rate responses.

302 rates of female vs. male flowering rather than bias in the underlying population composition  
303 (all sites were planted with equal numbers of females and males). Across sites and years, OSR  
304 variation was significantly predicted by [describe sex ratio analyses].<sup>8</sup>

## 305 Climate drivers of population viability across niche space

306 Putting all vital rates together in the MPM framework reveals how climate shapes fitness  
307 variation across niche dimensions and geographic space, and how accounting for sex structure  
308 modifies these inferences. Figure 3 shows the estimated probability of population viability  
309 ( $\lambda \geq 1$ ) across seasonal climate niche space; these probabilities account for uncertainty in the  
310 vital rate parameters as well as process error related to spatial heterogeneity and genotypic  
311 variation. For both female-dominant and two-sex models, fitness variation across niche space  
312 was dominated by temperature, with weaker effects of precipitation (compare vertical and  
313 horizontal contours in Fig. 3). These visual trends are supported by LTRE decomposition  
314 indicating that variation in fitness across climatic conditions is most strongly driven by  
315 responses to growing and dormant season temperature, with weaker interactive effects of  
316 precipitation that modulate the effects of temperature (Figure S-11). LTRE analysis also showed  
317 that declines in population viability at high and low temperatures were driven most strongly  
318 by reductions in vegetative growth and panicle production, with stronger contributions from  
319 females than males (Figure S-12).<sup>9</sup> Intermediate temperatures of both growing and dormant  
320 seasons were associated with near-certain projections of population viability ( $Pr(\lambda \geq 1) \approx 1$ ),  
321 and high and low temperature extremes during both seasons were associated with low niche  
322 suitability ( $Pr(\lambda \geq 1) < 0.2$ ). Higher precipitation slightly expanded the range of suitable  
323 temperatures during the dormant season (Fig. 3A), and the reverse was true in the growing  
324 season (Fig. 3B). Points in Fig. 3 show that climate change forecasted for the common  
325 garden locations would move many of them toward lower-suitability regions of niche space  
326 associated with high growing and dormant season temperatures (see also Fig. S-13).<sup>10</sup>

327 While the female-dominant and two-sex models were generally in agreement about  
328 high confidence in intermediate temperature optima, they differed around the edges of niche  
329 space (Fig. 3C,D<sup>11</sup>,S-13). The female-dominant model over-predicted population viability,  
330 especially with respect to growing season temperature. For example, the female-dominant

<sup>8</sup>I am not sure what the new sex ratio results look like, so not sure if we are keeping this.

<sup>9</sup>You can see here that I am suggesting we moved the lambda vs climate figure to an appendix. If you disagree we can keep it, but I think the niche space results are the better figure to show.

<sup>10</sup>I think we should redraw this without contours so that the points are more readable. I would also change the point types and sizes.

<sup>11</sup>All multi-panel figures need letter labels.

model predicted<sup>12</sup> that, for most levels of precipitation, warm average growing season (winter) temperatures of  $\sim 20^{\circ}\text{C}$  had high suitability ( $Pr(\lambda \geq 1) > 0.9$ ), while the two-sex model indicated that these conditions were most likely unsuitable ( $Pr(\lambda \geq 1) < 0.5$ ). Similarly, at low winter temperatures that the two-sex model identifies with high certainty as unsuitable ( $Pr(\lambda \geq 1) < 0.1$ ), the female-dominant model is more optimistic ( $Pr(\lambda \geq 1) > 0.4$ ). Across growing season climate space, the female-dominant model over-estimates population viability by ca. 10%, on average (Fig. 3D, Fig. S-14B). The difference between female-dominant and two-sex models was qualitatively similar but weaker in magnitude for niche dimensions of the dormant season (Fig. 3C, Fig. S-14A).

Female-dominant and two-sex models diverged most strongly in regions of niche space that favored strongly female-biased operational sex ratios (Fig. WE NEED A FIGURE FOR THIS). This suggests mate limitation as the biological mechanism underlying model differences. The two-sex model accounts for feedbacks between OSR and female fertility, with reduced seed viability at OSR exceeding  $\sim 75\%$  female panicles (Fig. WE NEED A FIGURE FOR THIS). Lacking this feedback, the female-dominant model over-predicts population viability in regions of niche space where male flowering is not sufficient to maximize seed set.

---

<sup>12</sup>I think I am switching tenses. We will need to clean this up.

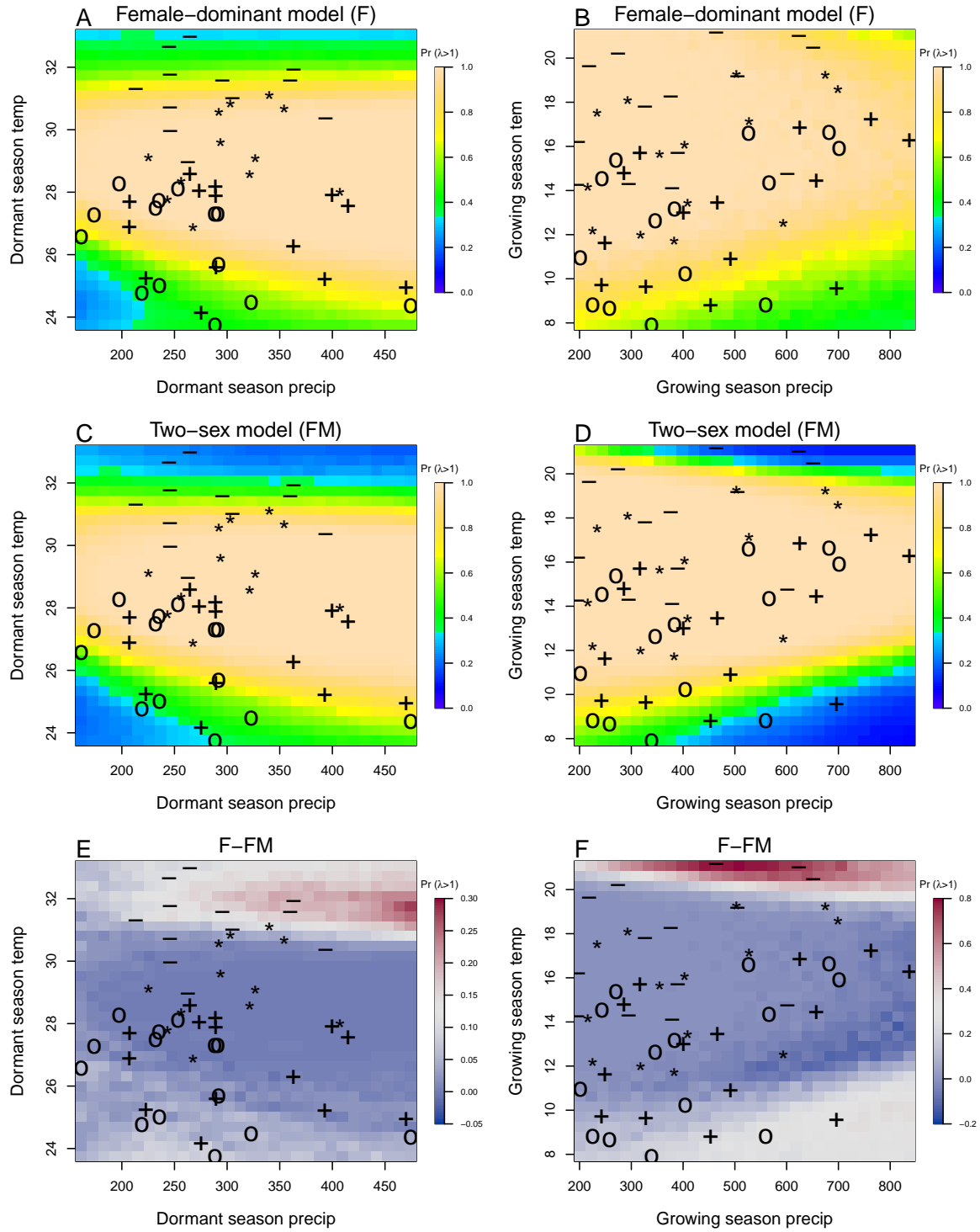


**Figure 3: A two-dimensional representation of the predicted niche shift over time (past, present and future climate conditions). "O": Past, "+" Current, "\*": RCP 4.5, "-": RCP 8.5.**

347 **Climatic change induces shifts in geographic niche and population OSR**

348 Projecting the climatic niche onto geographic space, we find that suitable niche conditions for  
349 Texas bluegrass are shifting north under climate change (Fig. 4). Under past (1901-1930) and  
350 present (1990-2019) conditions, the two-sex and female-dominant models predict widespread  
351 suitability with high confidence ( $Pr(\lambda \geq 1) \approx 1$ ) across much of Texas and Oklahoma. For  
352 both models, the predicted geographic niche generally corresponds well to independent  
353 observations of the Texas bluegrass distribution (Fig.<sup>13</sup>). The predicted geographic niche is  
354 more expansive than the observed distribution, particularly at southern, western, and eastern  
355 edges, suggesting some degree of range disequilibrium (e.g., due to dispersal limitation),  
356 geographic bias in occurrence observations, and/or model mis-specification. Comparing past  
357 to present conditions, the geographic niche for both models has shifted slightly poleward,  
358 with reductions in viability at the southern margins and expansions of viability at northern  
359 margins. The northward shift of suitable niche conditions is even more pronounced in  
360 projections to end-of-century (2071-2100) conditions, with the most dramatic changes in the  
361 most pessimistic (RCP8.5) scenario (Fig.<sup>14</sup>). In fact, under the pessimistic scenario, Texas  
362 bluegrass will have very little remaining climate suitability in the state of Texas by the end  
363 of the 21st century. The predicted poleward niche shift is consistent across different global  
364 circulation models (Figure S-15, Figure S-16, Figure S-17).

365 Female-dominant and two-sex models are in broad agreement about northward  
366 migration of the climatic niche, but the geographic projections reveal hotspots of disagreement  
367 where the female-dominant model over-predicts climate suitability and under-predicts the  
368 likelihood of range shifts (Fig. 4). These hotspots are generally regions of predicted female  
369 bias in the operational sex ratio (Fig. WE NEED A FIGURE FOR THIS.) The strongest contrast  
370 between the two models is in the pessimistic climate change scenario (RCP8.5), where the  
371 female-dominant model over-predicts population viability by ca. 25%<sup>15</sup> across much of the  
372 region (Fig. WE NEED A FIGURE SHOWING THE DISTRIBUTION OF THE DIFFERENCE)  
373 and under-estimates the magnitude of a potential range shift. In this scenario, a broad swath  
374 of the current distribution that is forecasted to be effectively unsuitable ( $Pr(\lambda \geq 1) \approx 0$ ) by the  
375 two-sex model is identified as marginally suitable ( $Pr(\lambda \geq 1) \approx 0.5$ ) by the female-dominant  
376 model. Accordingly, the OSR of Texas bluegrass across its range is projected to be ca. 75%  
377 female panicles, on average, by end of century under RCP8.5, an increase from ca. 60% female  
378 under projections for past and current conditions (Fig. 5). The more optimistic climate change  
379 scenario (RCP4.5) predicts an intermediate shift in OSR, with hotspots of change becoming

---

<sup>13</sup>I think we should add the GBIF records to the map.

<sup>14</sup>Here and throughout, we need to reference specific figure panels by letter label.

<sup>15</sup>I just eyeballed this. Real number should come from the histograms.

<sup>380</sup> strongly female-biased but most of the range remaining near current levels of 60% female  
<sup>381</sup> (Fig. 5; WE NEED A MAP SHOWING WHERE OSR IS BECOMING MORE BIASED).

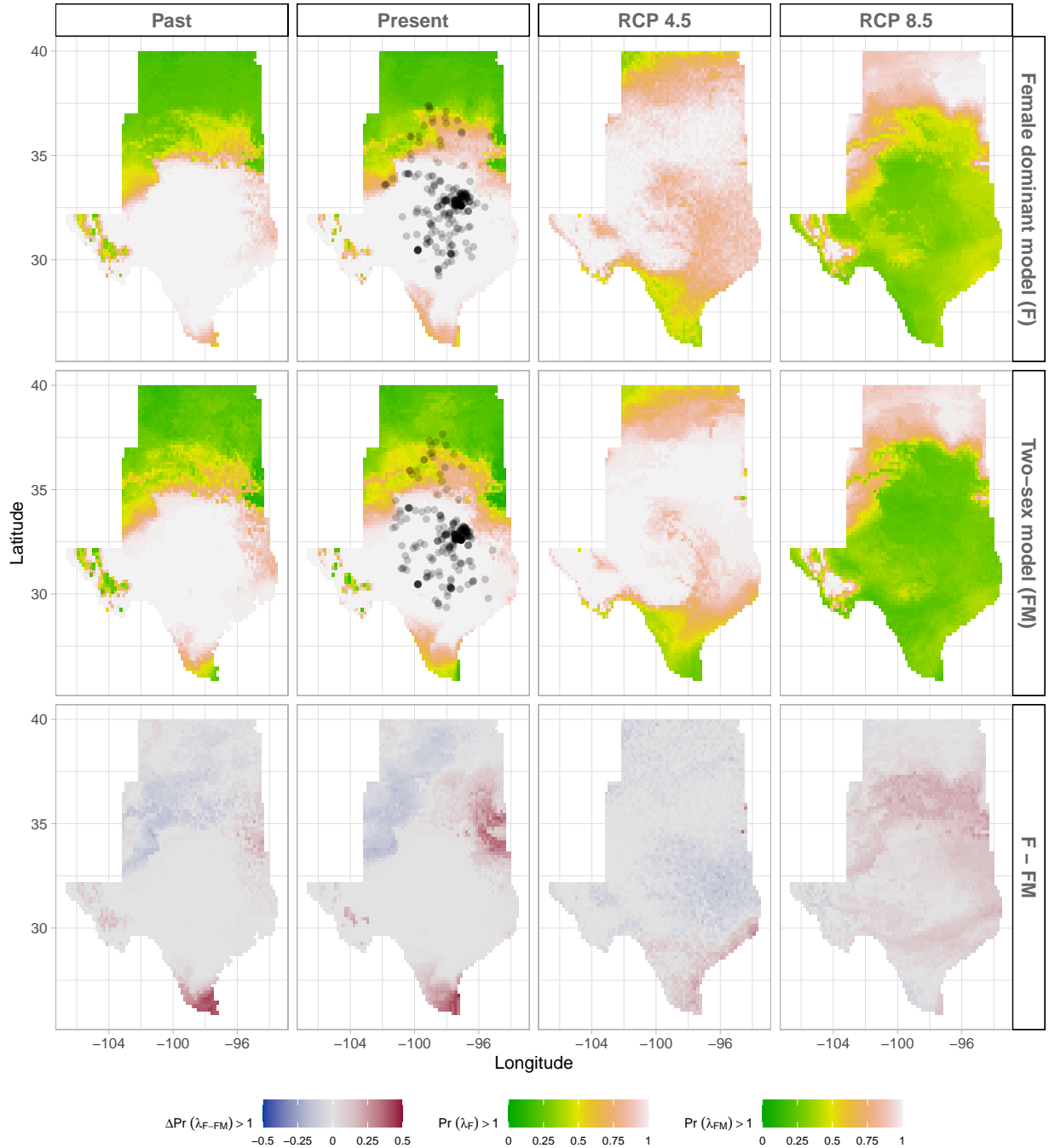


**Figure 4: Climate change favors range shift towards north edge.** (A) Past, (B) Current, (C and D) Future predicted range shift based on the predicted probabilities of self- sustaining populations,  $\text{Pr} (\lambda > 1)$ , using the two-sex model that incorporates sex- specific demographic responses to climate with sex ratio dependent seed fertilization. (E) Past, (F) Current, (G and H) Future predicted range shift based on the predicted probabilities of self- sustaining populations,  $\text{Pr} (\lambda > 1)$ , using the female dominant model. Future projections were based on the CMCC-CM model. The black dots on panel B and F indicate all known presence points collected from GBIF. The occurrences of GBIFs are distributed in with higher population fitness habitat  $\text{Pr} (\lambda > 1)$ , confirming that our study approach can reasonably predict range shifts.

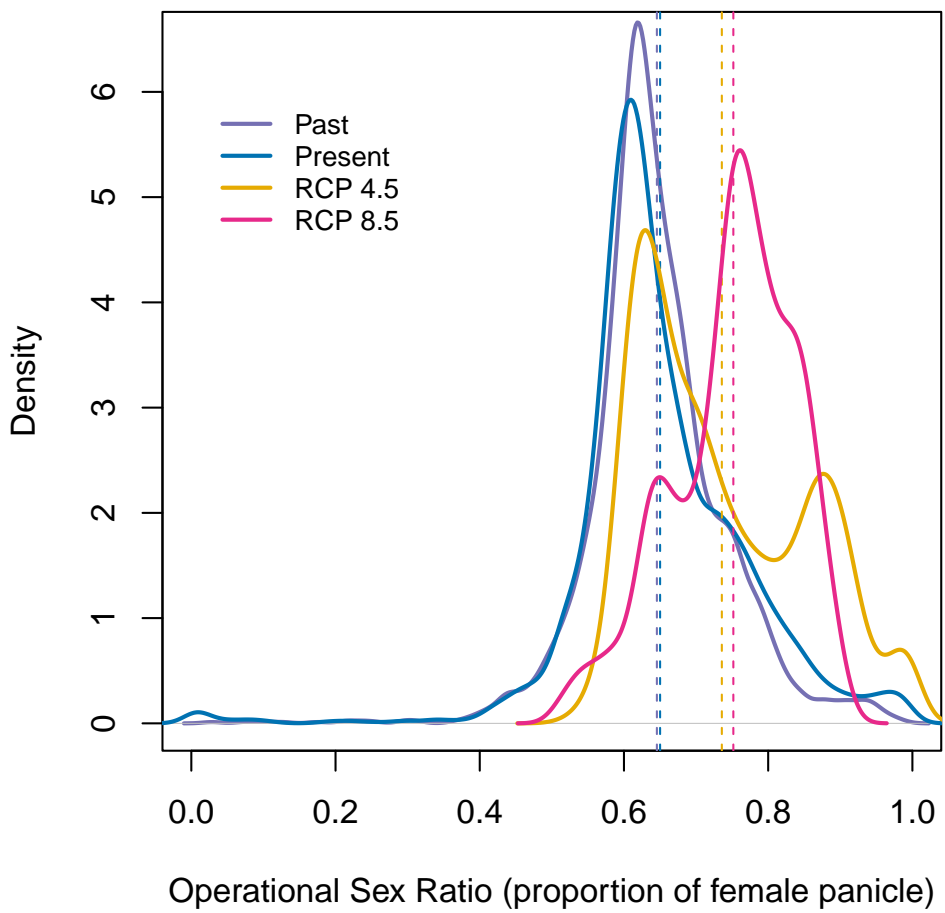


**Figure 5:** Change in Operational Sex Ratio (proportion of female panicle) over time (past, present, future). Future projections were based on the CMCC-CM model. The mean sex ratio for each time period is shown as vertical dashed line.

## 382 Discussion

383 Dioecious species make up a large fraction of Earth's biodiversity – most animals and many  
 384 plants – yet we have little knowledge about how sex-specific demography and responses to  
 385 climate drivers may affect population viability and range shifts of dioecious species under  
 386 climate change.<sup>16</sup> We used demographic data collected common garden experiments and  
 387 sex-structured demographic modeling to forecast for the first time the likely impact of climate  
 388 change on range dynamics of a dioecious species. Our future projections require extrapolation  
 389 to warmer or colder conditions than observed in our experiment and subsequently should be

---

<sup>16</sup>*Love this opening sentence.*

390 interpreted with caution (?).<sup>17</sup> Three general patterns emerged from our analysis of range-wide  
391 common garden experiments and sex-structured, climate-explicit demographic models. First,  
392 our Bayesian mixed effect model suggests a sex specific demographic response to climate  
393 change that lead to higher proportion of female as climate increase. Second, climate change  
394 favors a northern range shifts in suitable habitats. Third, the female dominant model (model  
395 that does not account for sex structure) overestimates species niche and range shifts.

396 There was a female demographic advantage leading to a female biased in response  
397 to climate change in *Poa arachnifera* populations. The extreme female-bias in response to  
398 climate change contrast with previous studies suggesting that an increase in male frequency  
399 in response to climate change (??). Two mechanisms could explain the observed demographic  
400 advantage of females over males for survival and flowering and the opposite for growth  
401 and number of panicles. The trade-off between fitness traits (survival, growth and fertility)  
402 due to resource limitation and the pollination mode of our study species (wind pollinated)  
403 could explain such a result (??). For most species, the cost of reproduction is often higher for  
404 females than males due to the requirement to develop seeds and fruits (?). However, several  
405 studies reported a higher cost of reproduction for males in wind pollinated species due to  
406 the larger amounts of pollen they produce (????).

407 Our results suggest that climate change will alter population at the center of the range and  
408 drive a northern range shifts. This impact of climate change on the species current niche could  
409 be explained by the increase of temperature over the next years. Small change in temperature  
410 of the growing and dormant season have a larger impact on population viability. Temperature  
411 can impact plant populations through different mechanisms. Increasing temperature could  
412 increase evaporative demand, affect plant phenology (???), and germination rate (?). The poten-  
413 tial for temperature to influence these different processes changes seasonally (?). For example,  
414 studies suggested that species that are active during the growing season such as cool grass  
415 species can have delayed phenology in response to global warming, particularly if temper-  
416 atures rise above their physiological tolerances (??). In addition, high temperature during the  
417 growing season by affecting pollen viability, fertilization could affect seed formation and germi-  
418 nation (??). Pollen dispersal may allow plants to resist climate change because pollen dispersal  
419 may provide the local genetic diversity necessary to adapt at the leading edge of the population  
420 (???). Since wind pollination is most effective at short distances, it is most often found in  
421 plant species growing at high density such as our study species, it is less likely that dispersal  
422 limitation affect niche shift in our study system. Difference in non-climatic factors such as soil,  
423 or biotic interactions could also explain decline in population growth rate as an indirect effects

---

17 I think extrapolation should be its own paragraph. This also relates to uncertainty in the climate forecasts.

424 of increase in temperature (??). For example, climate change could increase the strength of  
425 species competition and thereby constrain our study species to a narrower realized niche (??).

426 We found evidence of underestimation of the impact of climatic change on population  
427 dynamics by the female dominant model and implication for such an underestimation on  
428 conservation actions for dioecious species. The underestimation of the impact of climatic  
429 change on population dynamics by the female dominant model makes sense given the sex  
430 specific response to climatic change. *Poa arachnifera* populations will be female biased in  
431 response to climate change. That extreme female-bias could affect population growth rate by  
432 altering males' fitness with reduction on mate availability given that females individuals have a  
433 demographic advantage over males (??). Further, our work suggest that population viability is  
434 sensitive to climate under current and future conditions. This is key because most conservation  
435 actions are design from data on current responses to climate, rather than future response to  
436 climate (?). Since the role of male is not negligible in accurately predicting dioecious species  
437 response to climate change, management strategies that focus on both sexes would be effective  
438 and will enhance our understanding of dioecious species response to global warming.

## 439 Conclusion

440 We have investigated the potential consequence of skewness in sex ratio on population  
441 dynamics and range shift in the context of climate change using the Texas bluegrass. We  
442 found extreme female -biased in response to climate change. The effect of female biased  
443 will induce range shifts to the northern edge of the species current range by limiting mate  
444 availability. Beyond, our study case, our results also suggest that tracking only one sex could  
445 lead to an underestimation of the effect of climate change on population dynamics. Our  
446 work provides also a framework for predicting the impact of global warming on population  
447 dynamics using the probability of population to self-sustain.

## 448 Acknowledgements

449 This research was supported by National Science Foundation Division of Environmental  
450 Biology awards 2208857 and 2225027. We thank the institutions who hosted us at their field  
451 station facilities, including

# Supporting Information

## 452 S.1 Supporting Figures

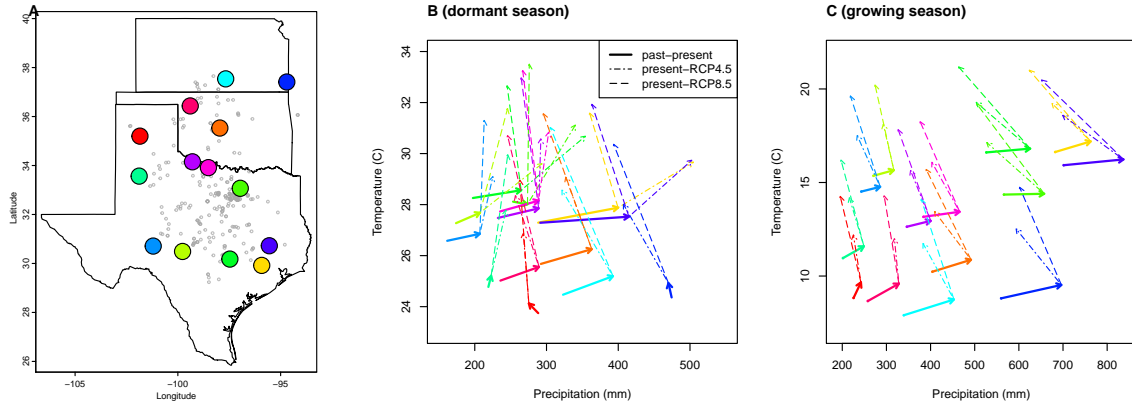


**Figure S-1:** (A), Common garden locations in Texas, Oklahoma, and Kansas (points) and (B,C) corresponding changes in growing and dormant season climate. Arrows in B,C connect past (1901-1930) and present (1990-2019) climate normals, and present and future (2071-2100) climate normals under RCP4.5 and RCP8.5 forecasts. Future forecasts are from MIROC5 but other climate models show similar patterns.

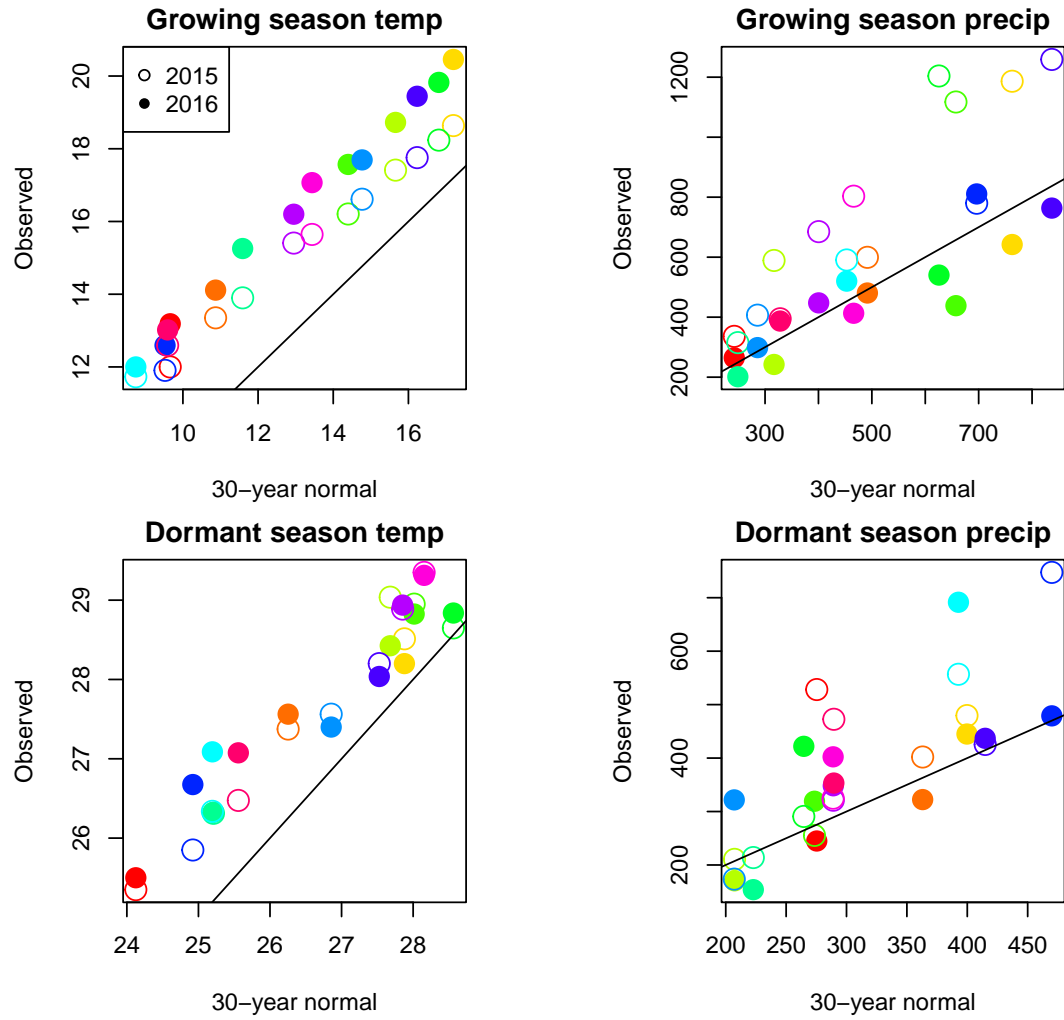


**Figure S-2:** Comparison of 30-year (1990-2019) climate normals and observed weather conditions at common garden sites during the 2014–15 and 2015–16 census periods. Temperature is in  $^{\circ}\text{C}$  and precipitation is in  $\text{mm}$ . Colors represent sites and lines show the  $y=x$  relationship.

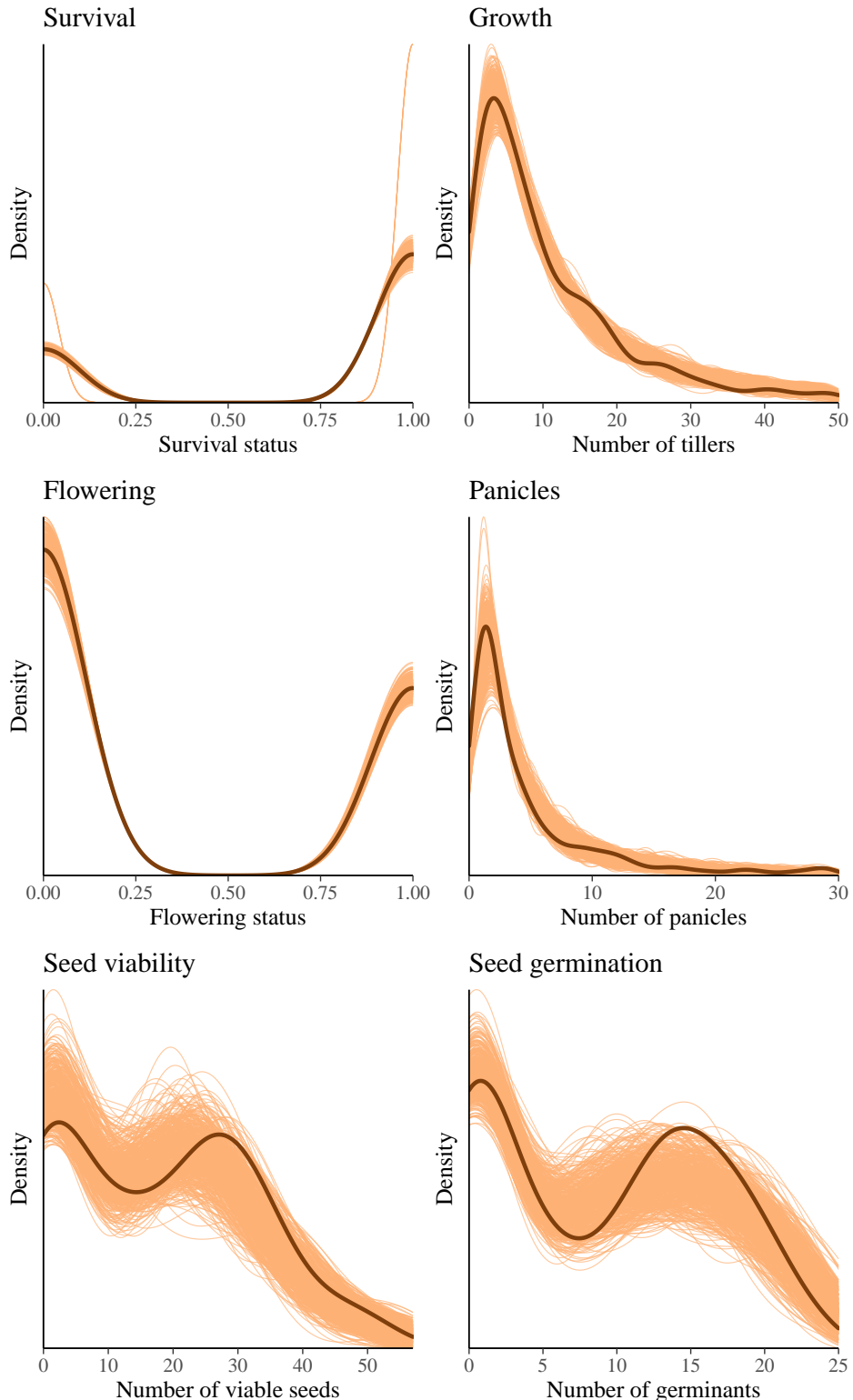


**Figure S-3:** Posterior predictive checks. Consistency between real data and simulated values suggests that the fitted vital rate models accurately describes the data. Graph shows density curves for the observed data (light orange) along with the simulated values (dark orange).

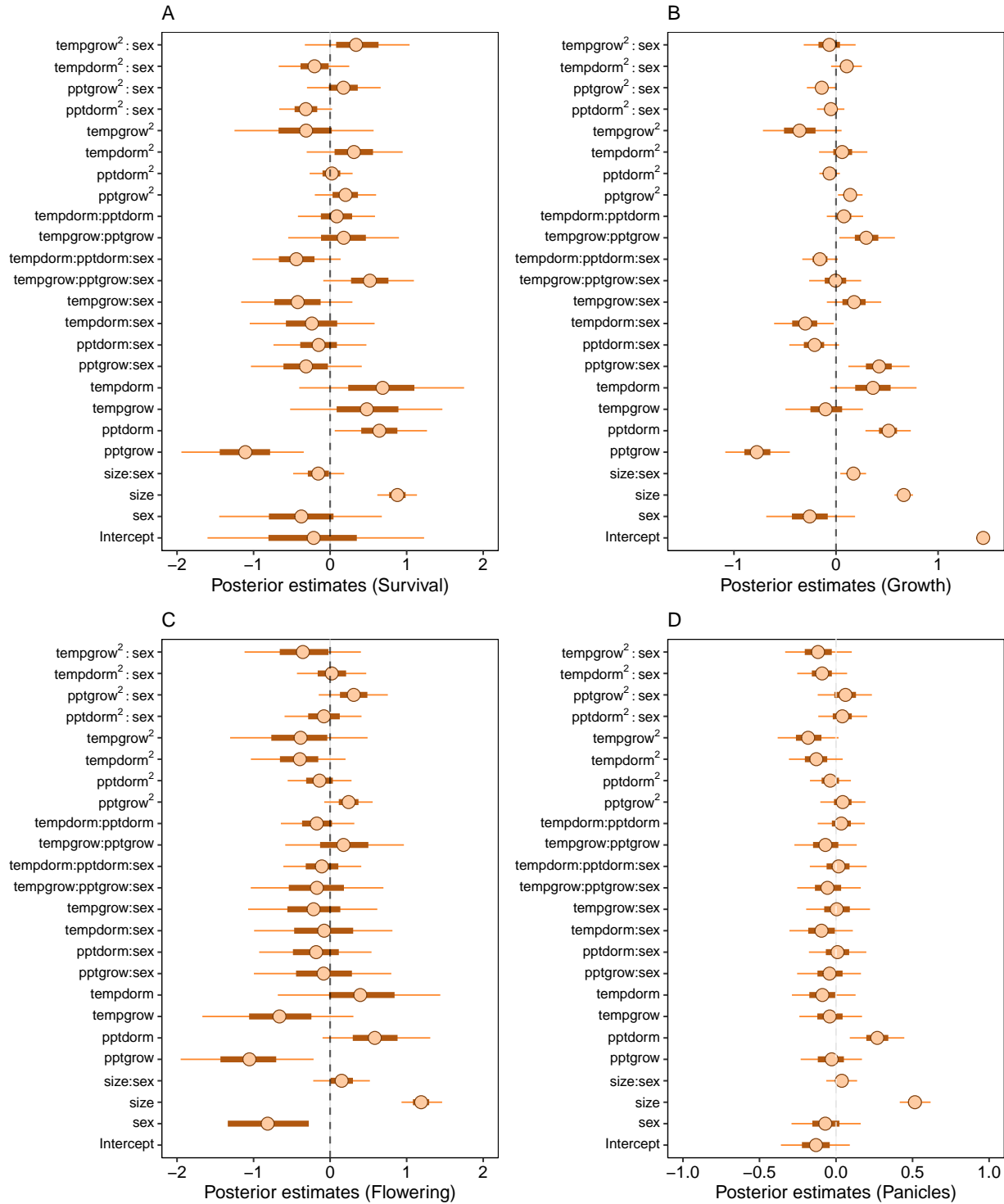


**Figure S-4:** Mean parameter values and 95% credible intervals of the posterior probability distributions. pptgrow is the precipitation of growing season, Tempgrow is the temperature of growing season, pptdorm is the temperature of dormant season, Tempdorm is the temperature of dormant season.

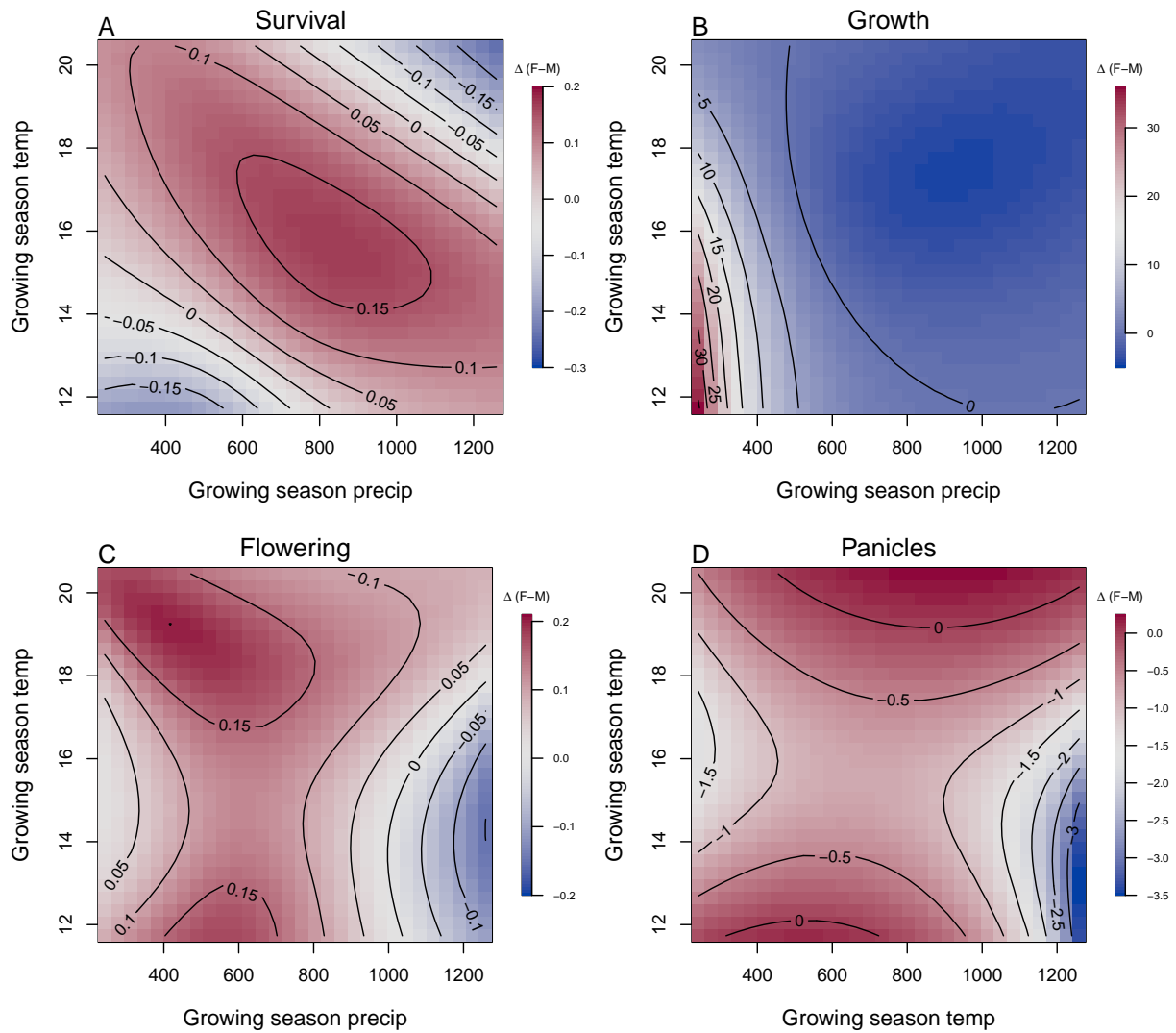


**Figure S-5:** Predicted difference in demographic response to climate across species range between female and male. Contours show predicted value of that difference conditional on precipitation and temperature of growing season

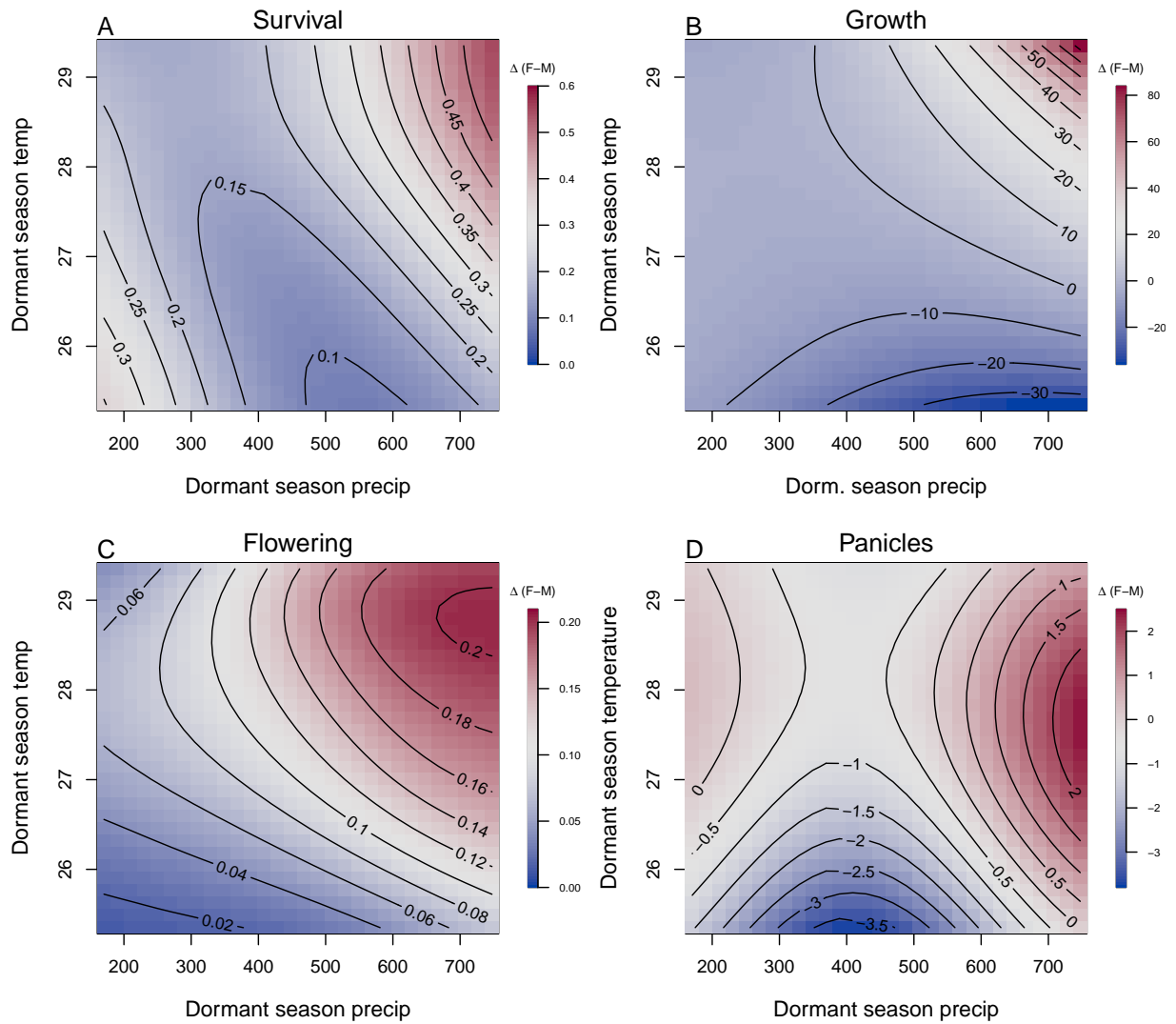


**Figure S-6:** Predicted difference in demographic response to climate across species range between female and male. Contours show predicted value of that difference conditional on precipitation and temperature of the dormant season

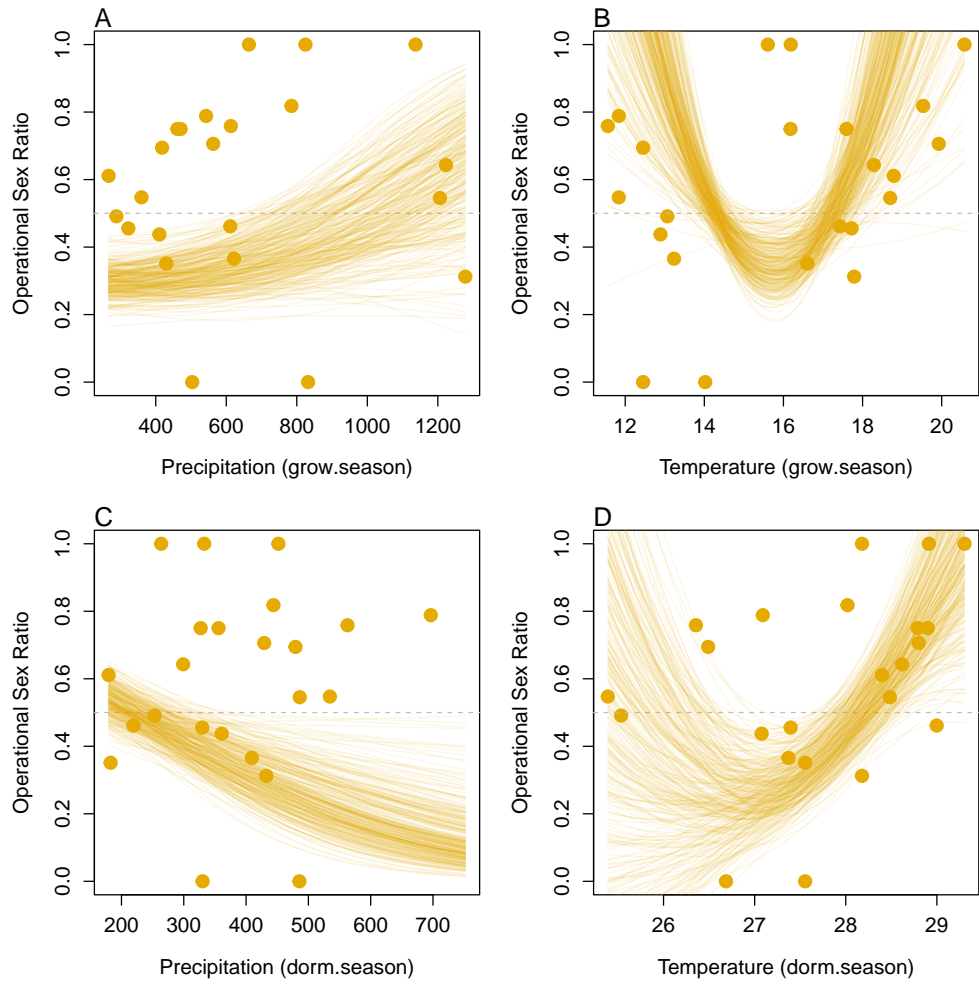


**Figure S-7: Significant Operational Sex Ratio response across climate gradient.** (A, B) Proportion of panicles that were females across precipitation and temperature of the growing season; (C, D) Proportion of panicles that were females across precipitation and temperature of the dormant season.

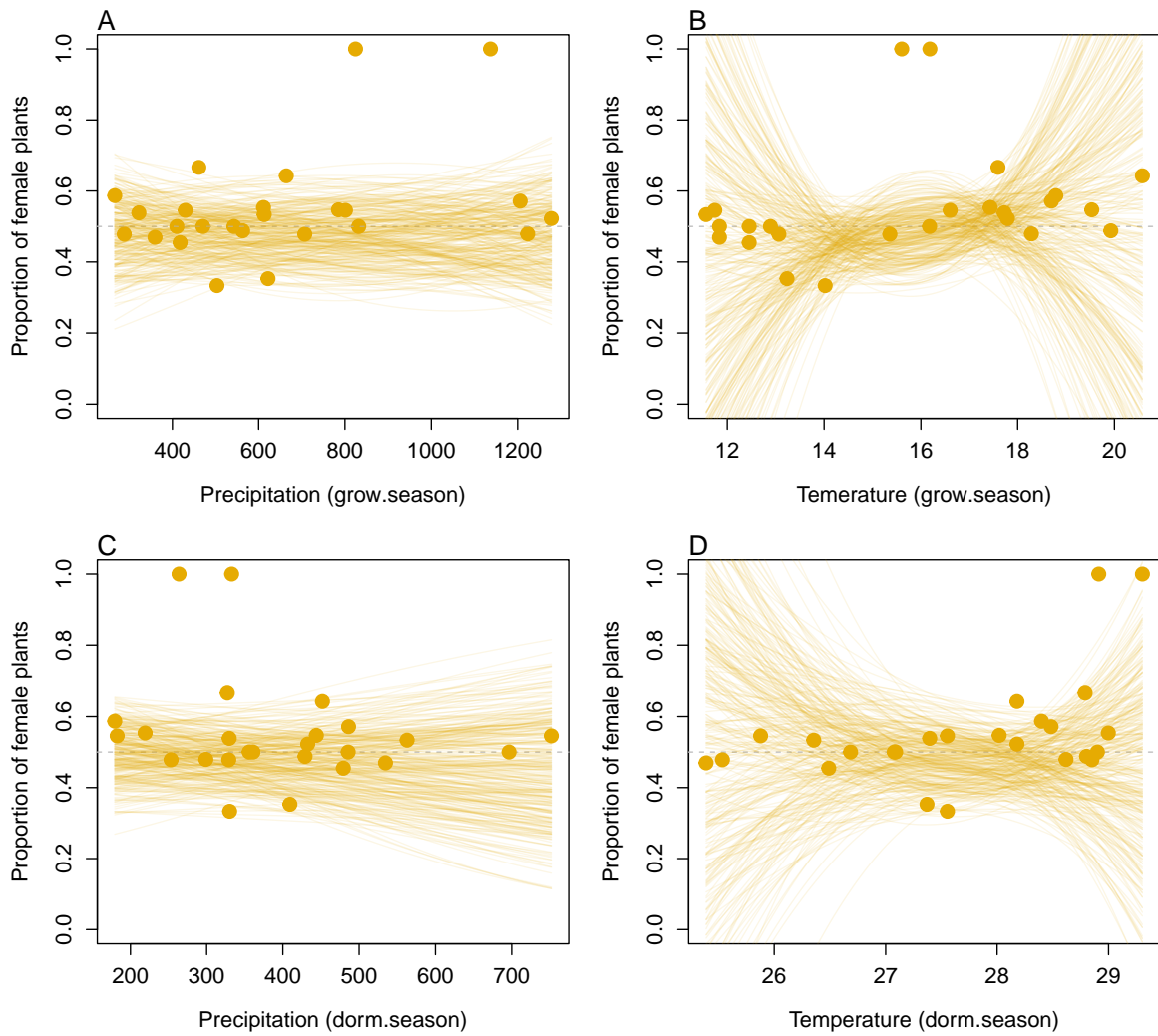


**Figure S-8: Variation in sex-ratio across climate gradient.** (A, B) Proportion of plants that were females across precipitation and temperature of the growing season; (C, D) Proportion of plants that were females across precipitation and temperature of the dormant season.

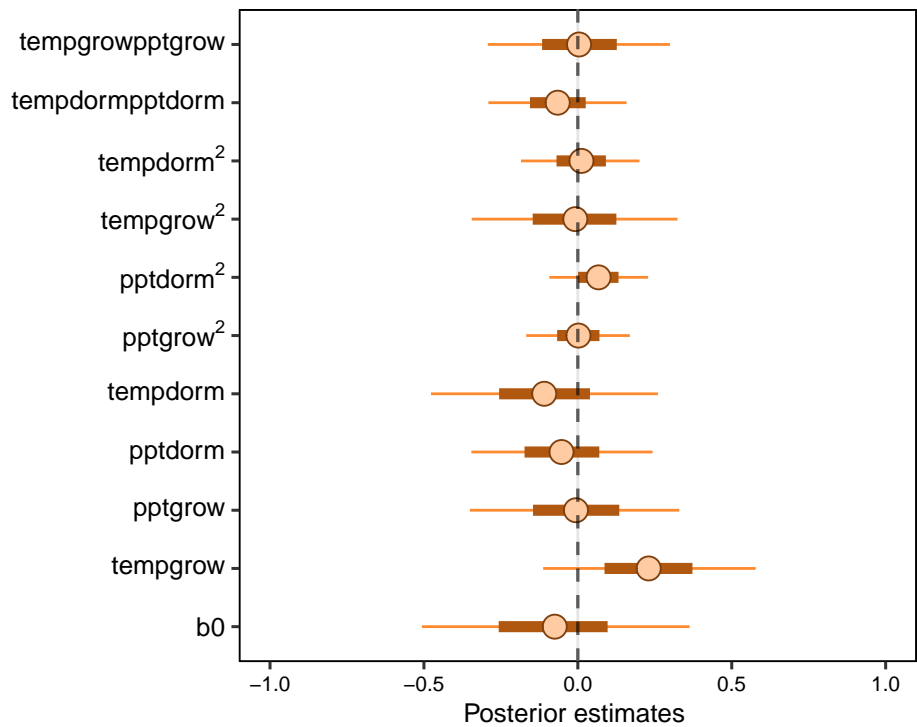


**Figure S-9:** Mean parameter values and 95% credible intervals of the posterior probability distributions. pptgrow is the precipitation of growing season, Tempgrow is the temperature of growing season, pptdorm is the temperature of dormant season, Tempdorm is the temperature of dormant season.

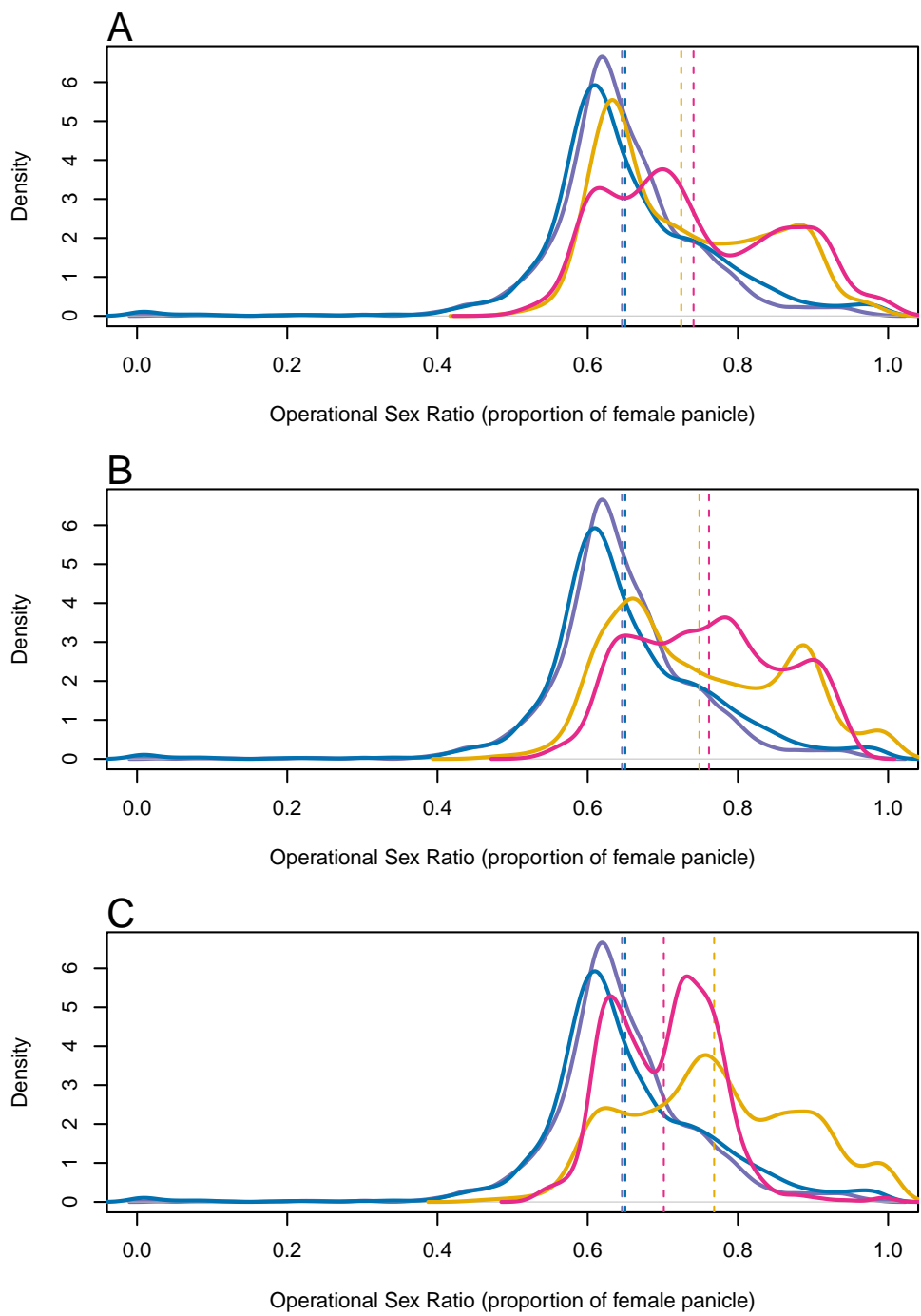


**Figure S-10:** Change in Operational Sex Ratio (proportion of female) over time (past, present, future). Future projections were based on A) MIROC 5, B) CES, C) ACC. The means for each model are shown as vertical dashed lines.

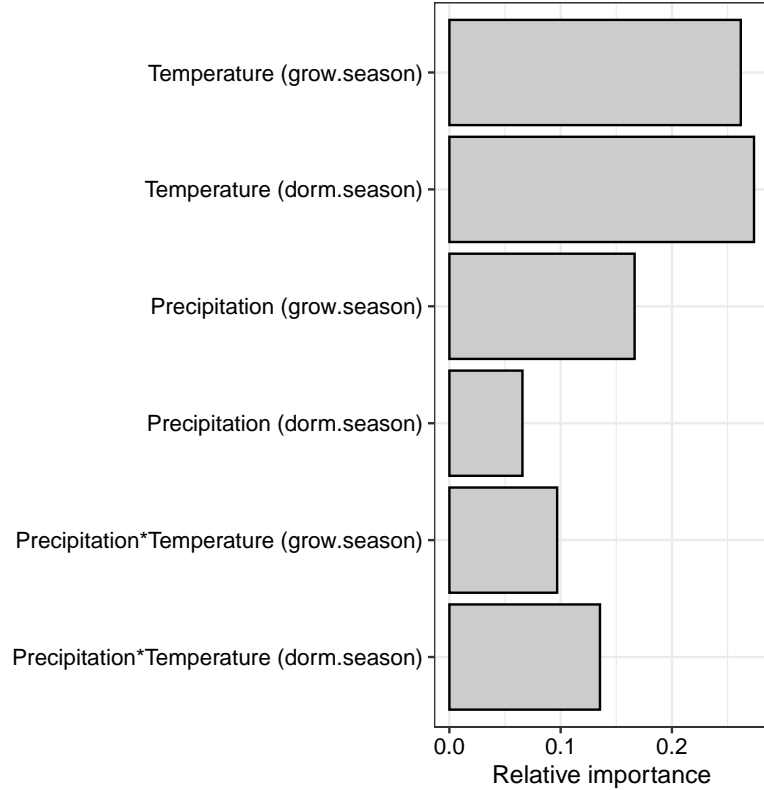


**Figure S-11:** Life Table Response Experiment: The bar represent the relative importance of each predictors.

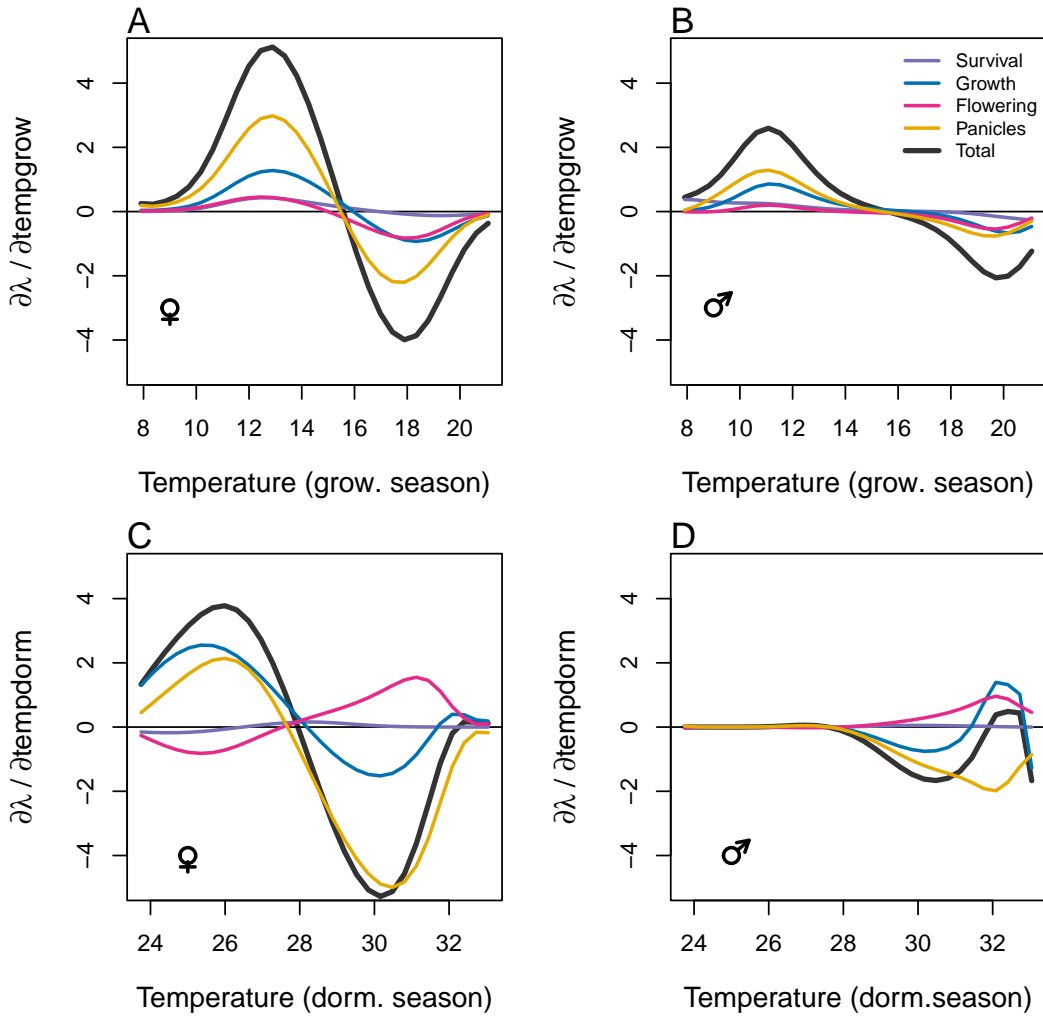


**Figure S-12:** Life table response experiment decomposition of the sensitivity of  $\lambda$  to seasonal climate into additive vital rate contributions of males and females based on posterior mean parameter estimates. (A) Temperature of growing season (contribution of female), (B) Temperature of growing season (contribution of male), (C) Temperature of dormant season (contribution of female) and (D) Temperature of dormant season (contribution of male).

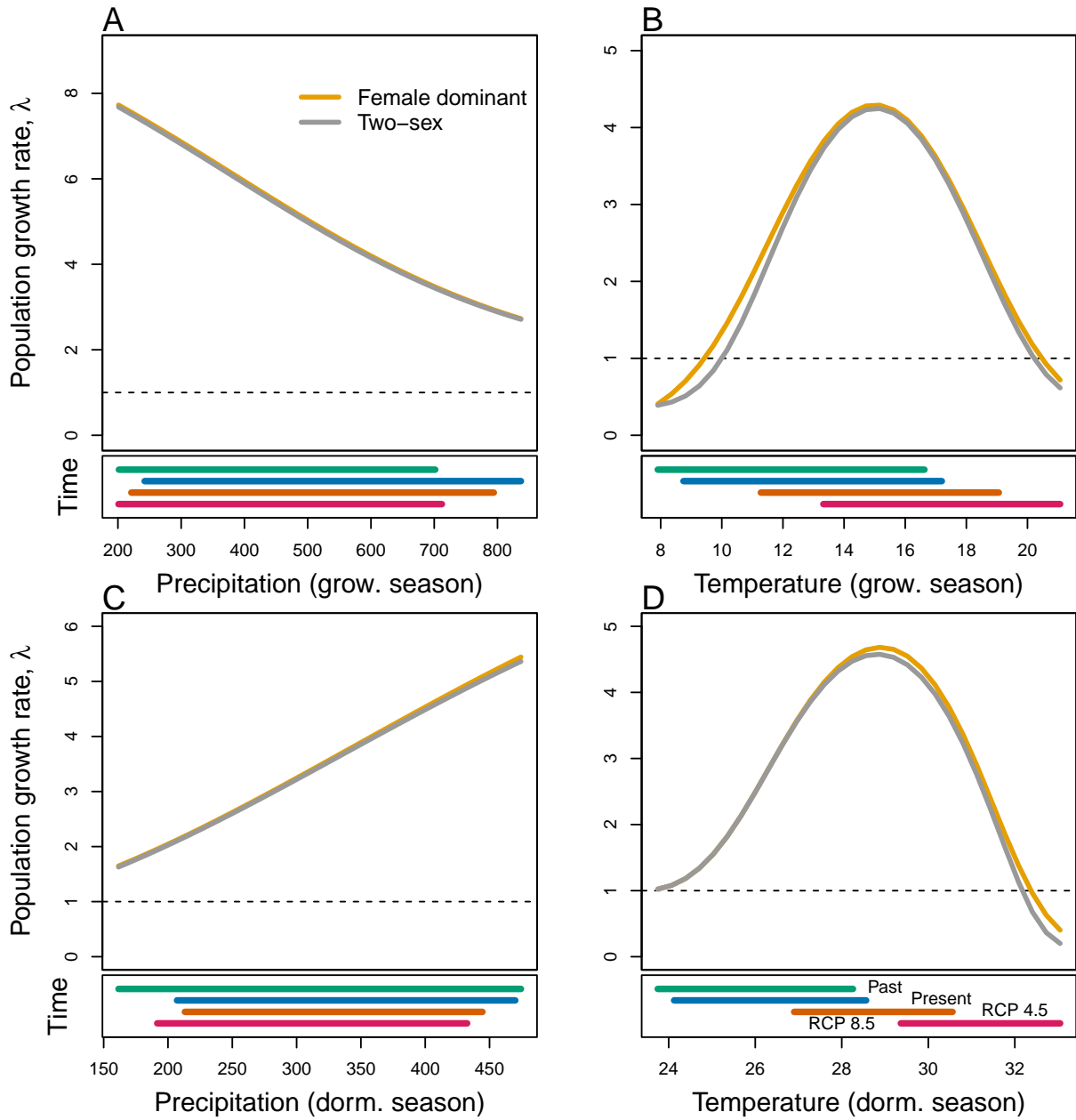


**Figure S-13: Predicted population growth rate ( $\lambda$ ) in different ranges of climate.** (A) Precipitation of the growing season, (B) Temperature of the growing season, (C) Precipitation of the dormant season, (D) Temperature of the dormant season. The grey curve shows prediction by the two-sex matrix projection model that incorporates sex-specific demographic responses to climate with sex ratio dependent seed fertilization. The orange curve represents the prediction by the female dominant matrix projection model. The dashed horizontal line indicates the limit of population viability ( $\lambda = 1$ ). Lower panels below each data panel show ranges of climate values for different time period (past climate, present and future climates). For future climate, we show a Representation Concentration Pathways (RCP) 4.5 and 8.5. Values of ( $\lambda$ ) are derived from the mean climate variables across 4 GCMs (MIROC5, ACCESS1-3, CESM1-BGC, CMCC-CM).

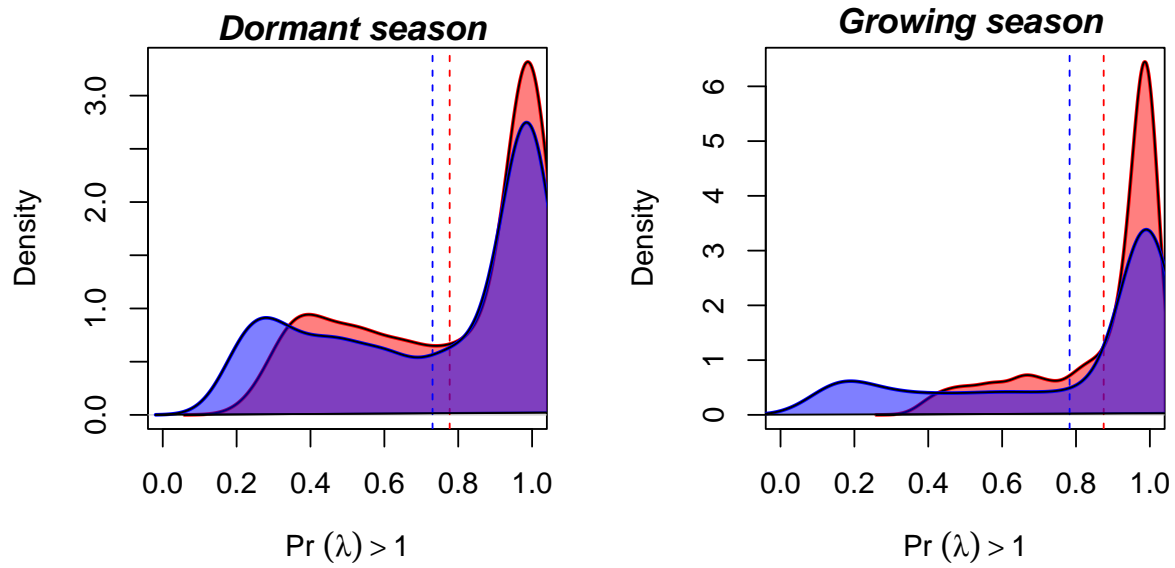


**Figure S-14:** Assessment of the statistical difference between the two-sex models and the female dominant model for the dormant and growing season. Plots show the density of  $\Pr(\lambda) > 1$  values for female dominant (pink) and two-sex models (violet) for each season. The means for each model are shown as vertical dashed lines.

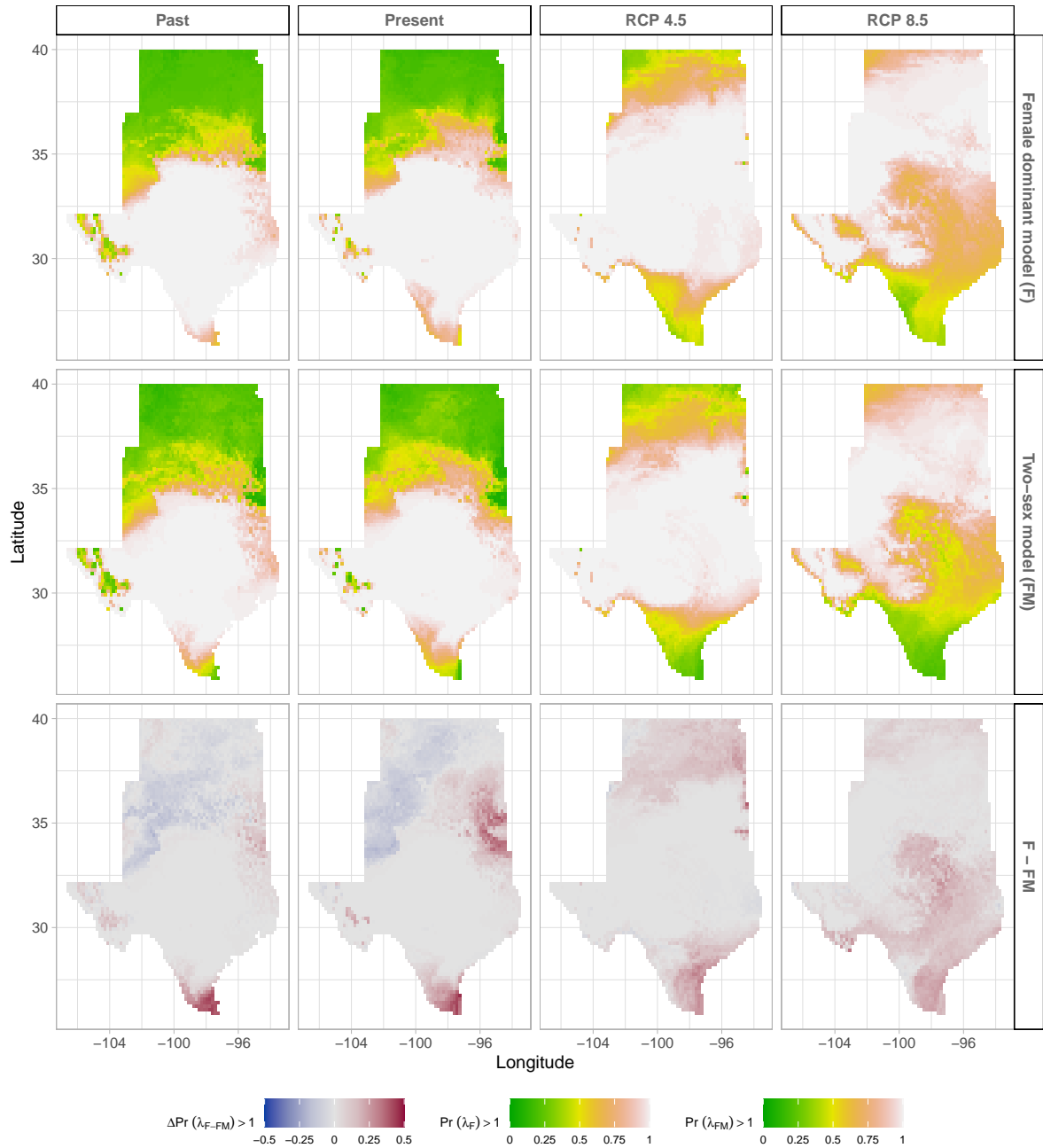


**Figure S-15:** Climate change favors range shift toward the North edge of the current range. (A) Past, (B) Current, (C and D) Future predicted range shift based on the predicted probabilities of self- sustaining populations,  $\Pr(\lambda > 1)$ , using the two-sex model that incorporates sex- specific demographic responses to climate with sex ratio dependent seed fertilization. (E) Past, (F) Current, (G and H) Future predicted range shift based on the predicted probabilities of self- sustaining populations,  $\Pr(\lambda > 1)$ , using the female dominant model. Future projections were based on the CESM1-BGC model. The black dots on panel B and F indicate all known presence points collected from GBIF from 1990 to 2019, which corresponds to the current condition in our prediction. The occurrences of GBIFs are distributed in with higher population fitness habitat  $\Pr(\lambda > 1)$ , confirming that our study approach can reasonably predict range shifts.

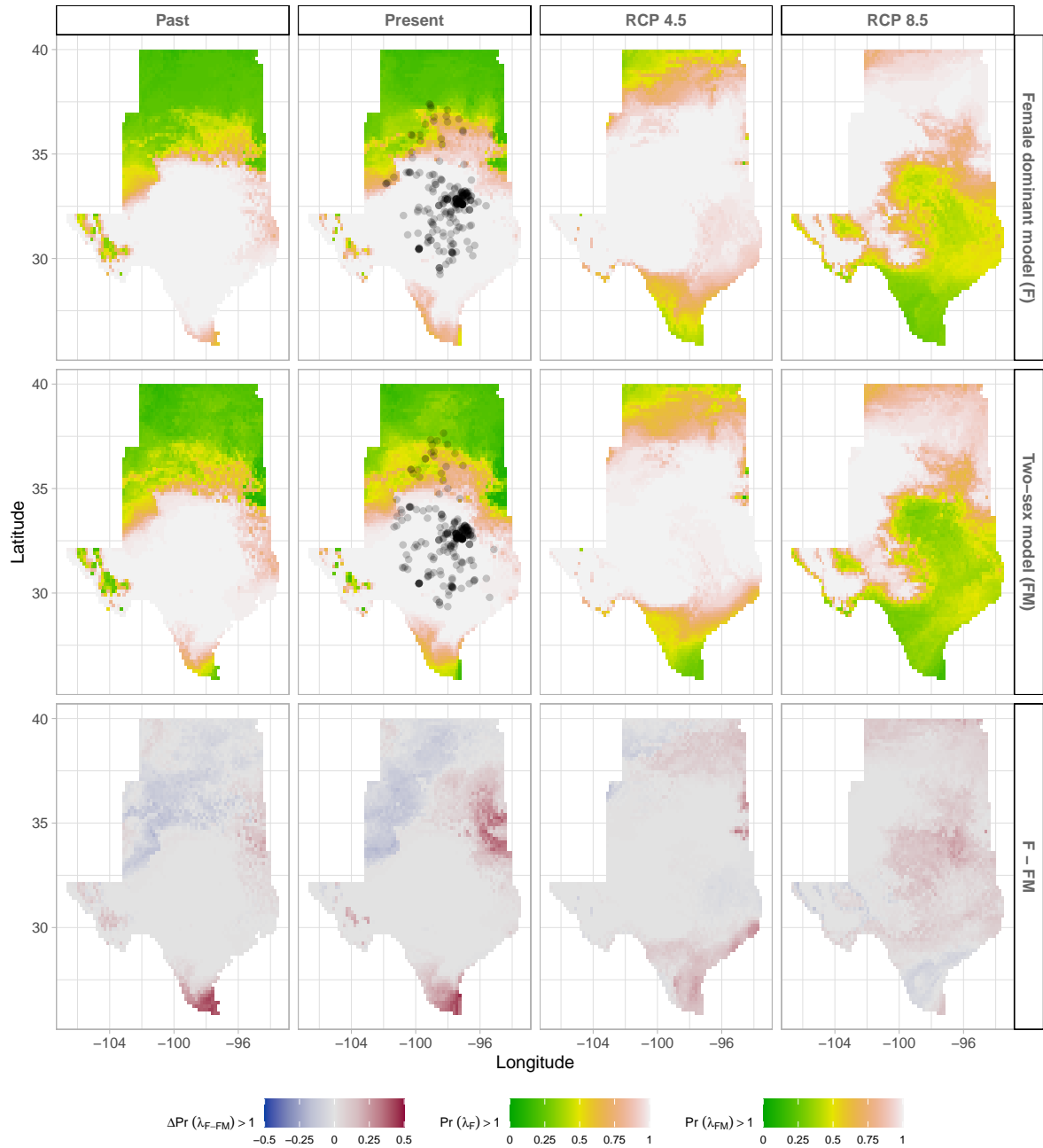


**Figure S-16:** Climate change favors range shift toward the North edge of the current range. (A) Past, (B) Current, (C and D) Future predicted range shift based on the predicted probabilities of self-sustaining populations,  $\Pr(\lambda > 1)$ , using the two-sex model that incorporates sex-specific demographic responses to climate with sex ratio dependent seed fertilization. (E) Past, (F) Current, (G and H) Future predicted range shift based on the predicted probabilities of self-sustaining populations,  $\Pr(\lambda > 1)$ , using the female dominant model. Future projections were based on the ACCESS model. The black dots on panel B and F indicate all known presence points collected from GBIF from 1990 to 2019, which corresponds to the current condition in our prediction. The occurrences of GBIFs are distributed in with higher population fitness habitat  $\Pr(\lambda > 1)$ , confirming that our study approach can reasonably predict range shifts.

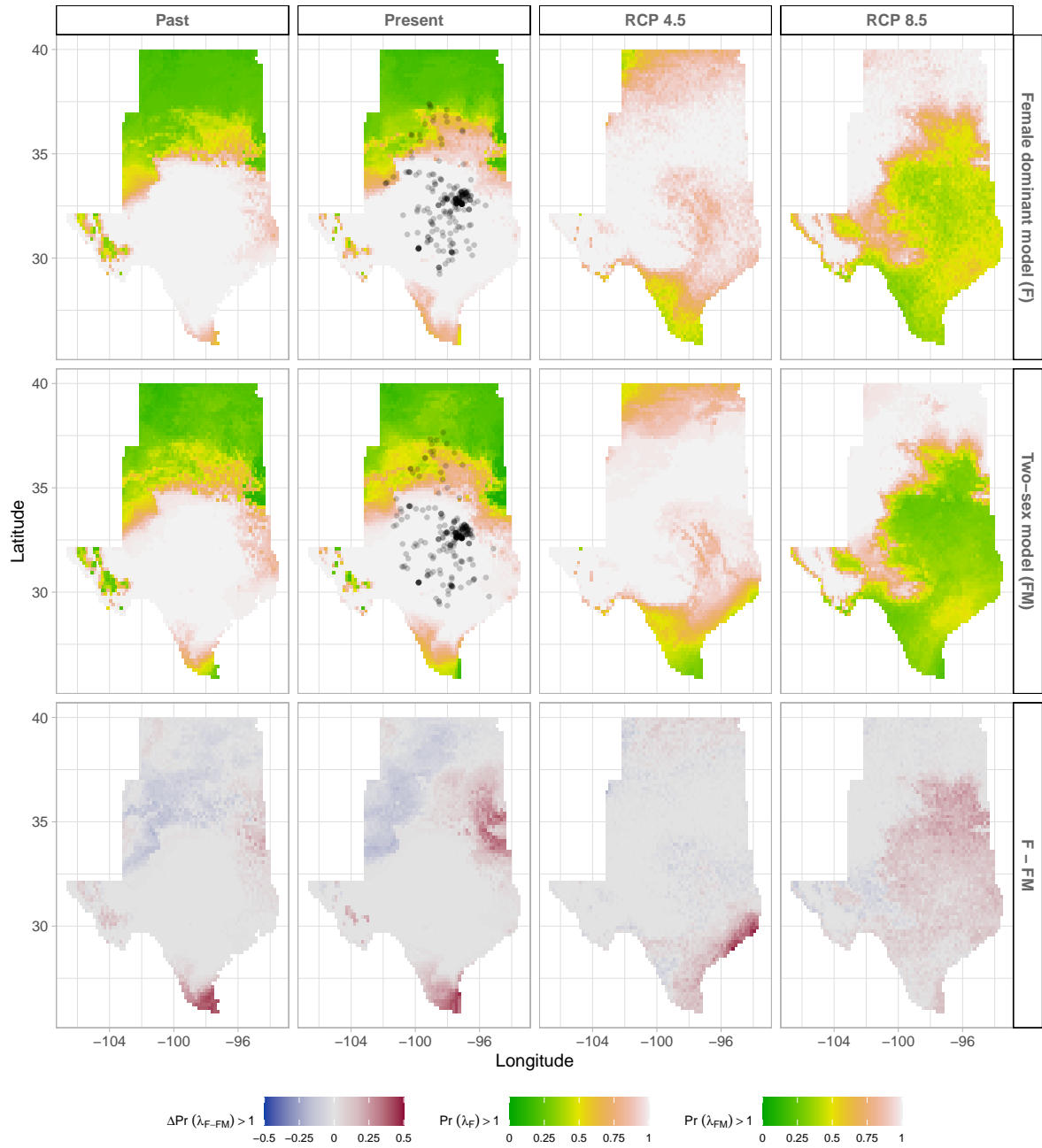


**Figure S-17:** Climate change favors range shift toward the North edge of the current range. (A) Past, (B) Current, (C and D) Future predicted range shift based on the predicted probabilities of self- sustaining populations,  $\Pr(\lambda > 1)$ , using the two-sex model that incorporates sex- specific demographic responses to climate with sex ratio dependent seed fertilization. (E) Past, (F) Current, (G and H) Future predicted range shift based on the predicted probabilities of self- sustaining populations,  $\Pr(\lambda > 1)$ , using the female dominant model. Future projections were based on the MIROC5 model. The black dots on panel B and F indicate all known presence points collected from GBIF from 1990 to 2019, which corresponds to the current condition in our prediction. The occurrences of GBIFs are distributed in with higher population fitness habitat  $\Pr(\lambda > 1)$ , confirming that our study approach can reasonably predict range shifts.

453 **S.2 Supporting Methods**

454 **S.2.1 Sex-specific demographic responses to climatic variation across  
455 common garden sites**

456 Vital rate models were fit with the same linear predictors for the expected value ( $\mu$ )(Eq.S.1):

$$\begin{aligned} \mu = & \beta_0 + \beta_1 size + \beta_2 sex + \beta_3 pptgrow + \beta_4 pptdorm + \beta_5 tempgrow + \beta_6 tempdorm \\ & + \beta_7 pptgrow * sex + \beta_8 pptdorm * sex + \beta_9 tempgrow * sex + \beta_{10} tempdorm * sex \\ & + \beta_{11} size * sex + \beta_{12} pptgrow * tempgrow + \beta_{13} pptdorm * tempdorm \\ & + \beta_{14} pptgrow * tempgrow * sex + \beta_{15} pptdorm * tempdorm * sex + \beta_{16} pptgrow^2 \\ & + \beta_{17} pptdorm^2 + \beta_{18} tempgrow^2 + \beta_{19} tempdorm^2 + \beta_{20} pptgrow^2 * sex \\ & + \beta_{21} pptdorm^2 * sex + \beta_{22} tempgrow^2 * sex + \beta_{23} tempdorm^2 * sex + \phi + \rho + \nu \end{aligned} \quad (S.1)$$

458 where  $\beta_0$  is the grand mean intercept,  $\beta_1$  is the size dependent slopes. *size* was on a natural  
459 logarithm scale.  $\beta_2 \dots \beta_{13}$  represent the climate dependent slopes.  $\beta_{14} \dots \beta_{23}$  represent the  
460 sex-climate interaction slopes. *pptgrow* is the precipitation of the growing season, *tempgrow*  
461 is the temperature of the growing season, *pptdorm* is the precipitation of the dormant season,  
462 *tempdorm* is the temperature of the dormant season.

463 **S.2.2 Sex ratio responses to climatic variation across common garden sites**

464 To understand the impact of climatic variation across common garden sites on sex ratio, OSR  
465 and SR models using the same linear predictors for the expected value ( $\nu$ )(Eq.S.2):

$$\begin{aligned} \nu = & \omega_0 + \omega_1 pptgrow + \omega_2 pptdorm + \omega_3 tempgrow + \omega_4 tempdorm + \\ & \omega_5 pptgrow^2 + \omega_6 pptdorm^2 + \omega_7 tempgrow^2 + \omega_8 tempdorm^2 + \epsilon \end{aligned} \quad (S.2)$$

467 where OSR is the proportion of panicles that were female or proportion of female individuals  
468 in the experimental populations, c is the climate.  $\omega_0$  is the intercept,  $\omega_1, \dots, \omega_8$  are the climate  
469 dependent slopes.  $\epsilon$  is error term.

470 **S.2.3 Sex ratio experiment**

471 To estimate the probability of seed viability, the germination rate and the effect of sex-ratio  
472 variation on female reproductive success, we conducted a sex-ratio experiment at one site  
473 near the center of the range to estimate the effect of sex-ratio variation on female reproductive

success. The details of the experiment are provided in ? and ?. Here we provide a summary of the experiment. We established 124 experimental populations in plots measuring 0.4 x 0.4m and separated by at least 15m from each other. We varied population density (1-48 plants/plot) and sex ratio (0%-100% female) across the experimental populations, and we replicated 34 combinations of density and sex ratio. We collected panicles from a subset of females in each plot and recorded the number of seeds in each panicle. We assessed reproductive success (seeds fertilized) using greenhouse-based germination and trazolium-based seed viability assays. Seed viability was modeled with a binomial distribution where the probability of viability ( $v$ ) was given by:

$$v = v_0 * (1 - OSR^\alpha) \quad (\text{S.3})$$

where  $OSR$  is the proportion of panicles that were female in the experimental populations.  $\alpha$  is the parameter that control for how viability declines with increasing female bias. Further, germination rate was modeled using a binomial distribution to model the germination data from greenhouse trials. Given that germination was conditional on seed viability, the probability of success was given by the product  $v*g$ , where  $v$  is a function of  $OSR$  (Eq. S.3) and  $g$  is assumed to be constant.